Electronic Supplementary Information (ESI) for ***Polymer Chemistry***
This journal is © The Royal Society of Chemistry 2018

Pot- and atom-economic synthesis of oligomeric non-fullerene acceptors *via* C–H direct arylation

Li-Hong Wang,[‡a] Xian-Jie Chen,[‡b] Dong-Nai Ye,[a] Hui Liu,[a] Yan Chen,[a] Ai-Guo Zhong,[c] Chang-Zhi Li,[*b] and Shi-Yong Liu [*a]

[a] College of Materials, Metallurgical and Chemistry, Jiangxi University of Science and Technology, Ganzhou 341000, P. R. China

[b] Department of Polymer Science and Engineering, Zhejiang University, Hangzhou 310027 (P. R. China)

[c] Department of Pharmacy & Chemistry, Taizhou University, 317000, PR China

Corresponding author:

* E-mail: chelsy@jxust.edu.cn (S. -Y. Liu), czli@zju.edu.cn (C.-Z. Li)

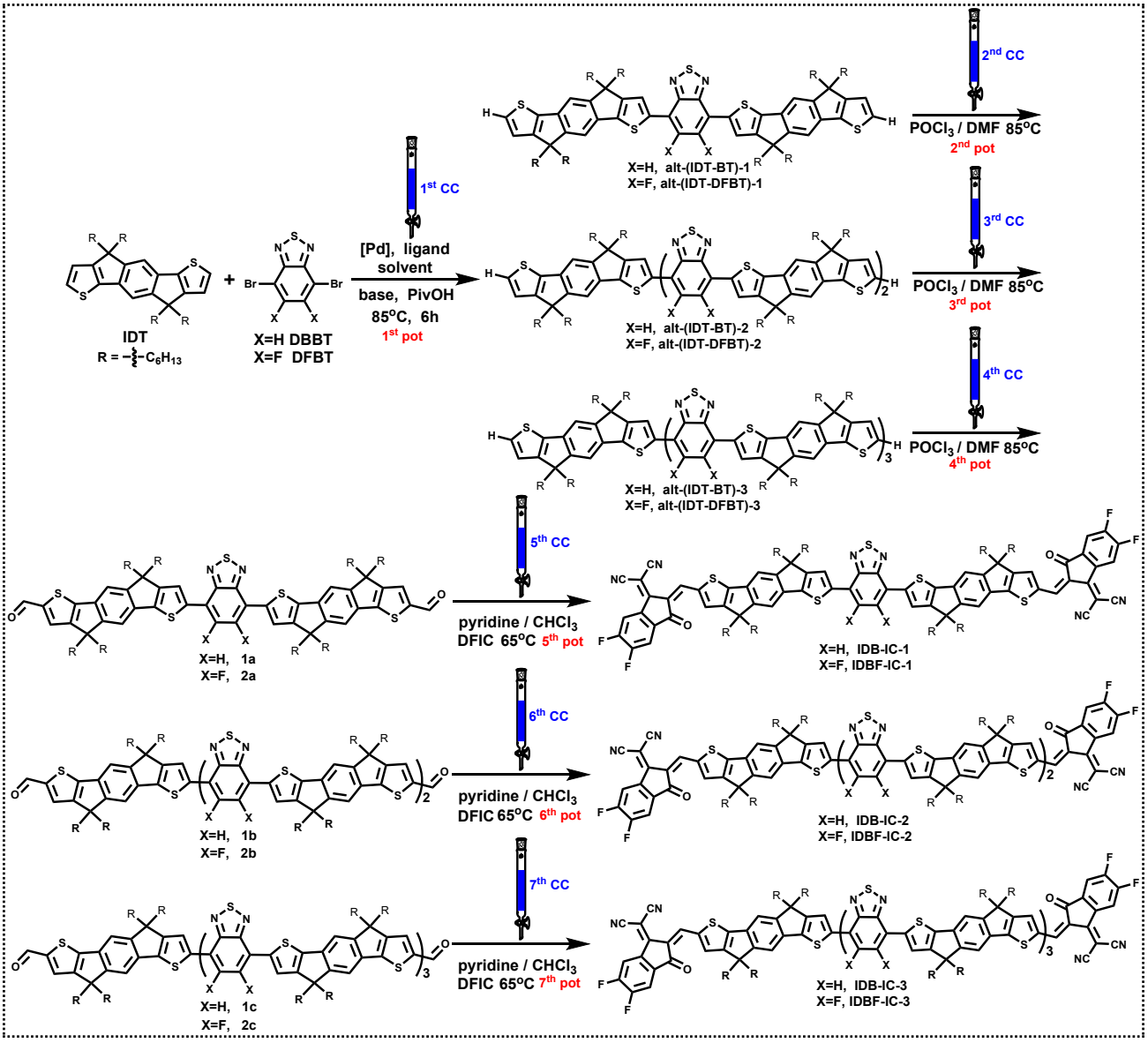

Scheme S1 Synthesis of IDB-IC-n or IDBF-IC-n (n = 1~3) *via* the conventional one-by-one strategy.

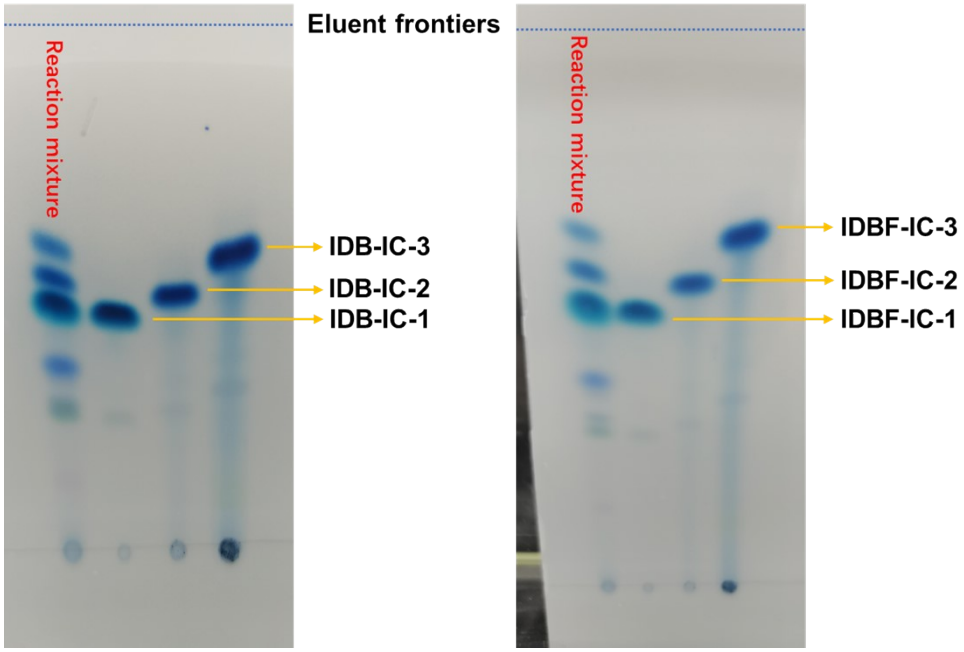

Fig. S1 Thin-layer chromatography (TLC) analysis for the reaction mixture of last pot of Knovenagel reaction in **Scheme 1** [The starting spots on each TLC plate involved the reaction mixture and their corresponding purified NFAs, i.e., IDB-IC-n (left plate) and IDBF-IC-n (right plate) using CH_2Cl_2: hexane (1.2:1, v/v) as developing solvent].

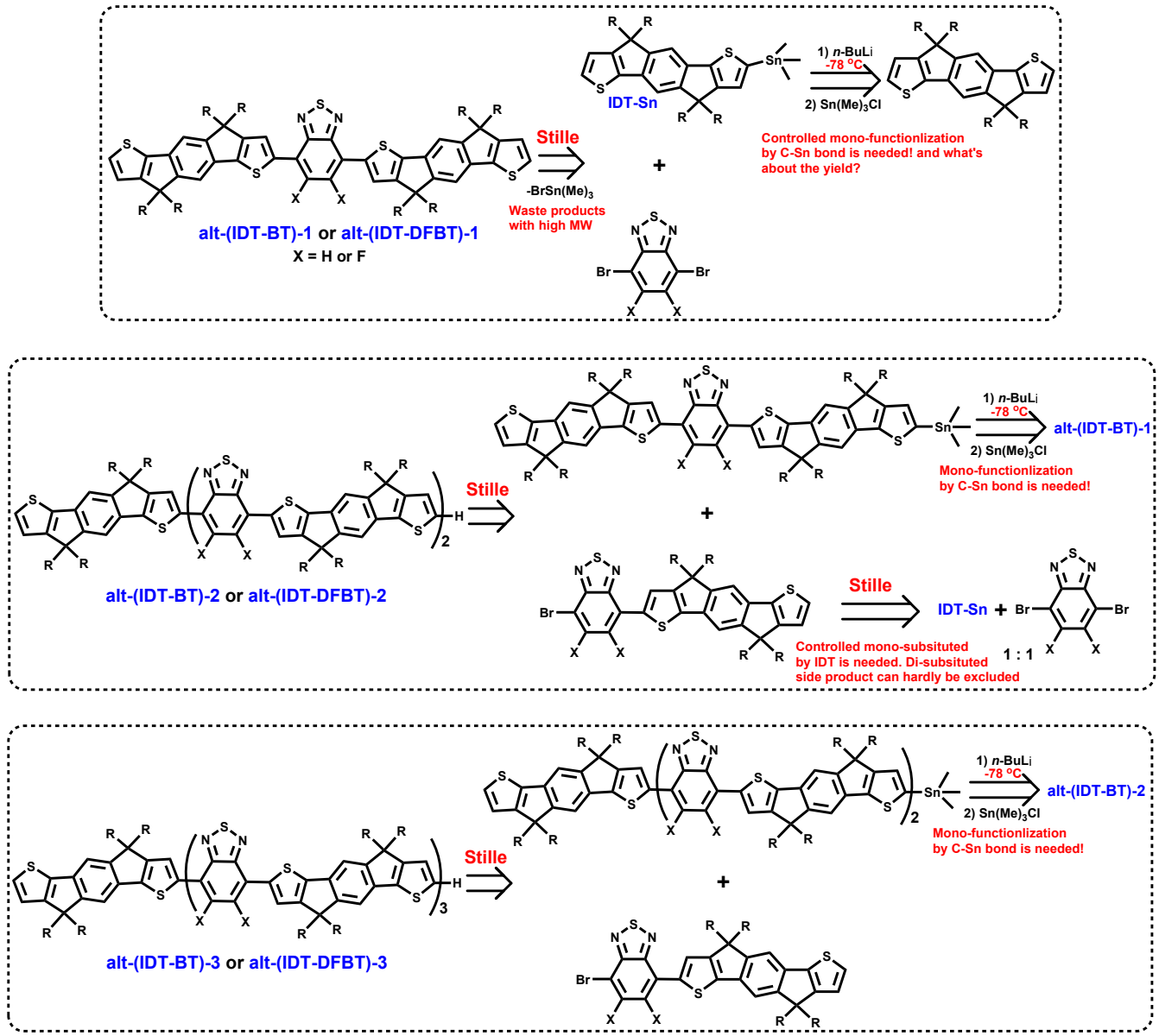

Scheme S2 Retrosynthetic analysis of alt-(IDT-BT)-n or alt-(IDT-DFBT)-n (n = 1~3) *via* classical Stille coupling reaction. [Compared to C–H oligomerization we developed, much more synthetic steps and harsh reaction conditions (for highly active BuLi) will be involved if Stille coupling is employed instead, including controlled mono-functionalization of intermediates by C–Sn bond, low reaction temperature (-78 °C) with anhydrous condition, and controlled mono-substituted of DBBT (or DFBT) by IDT.]

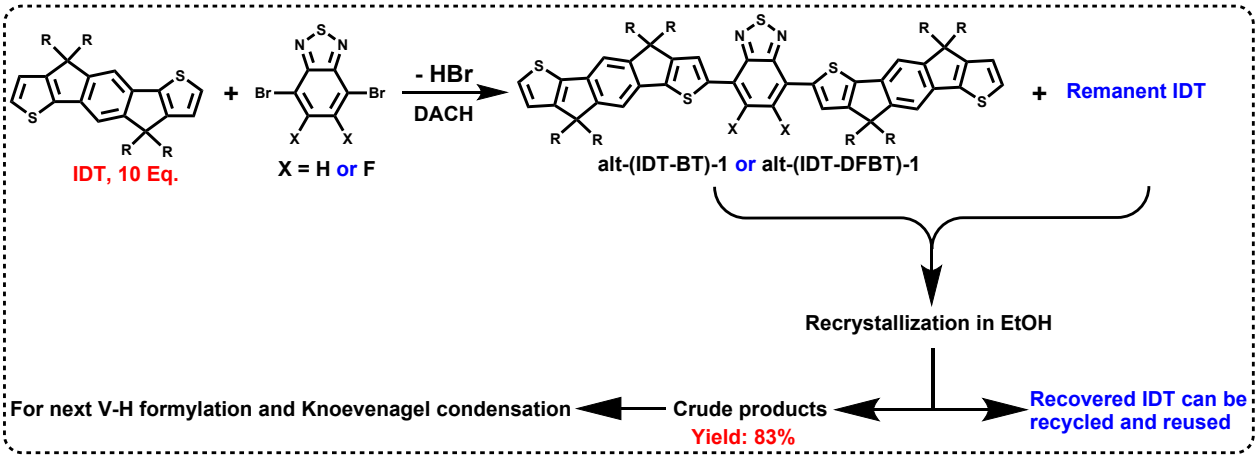

Scheme S3 Non-equimolar C–H arylation coupling (10 : 1) between IDT and DBBT (or DFBT). [After completing reaction, the mixtures were subjected to recrystallization in EtOH to separate products, *i.e.*, alt-(IDT-BT)-1 or alt-(IDT-DFBT)-1, and the excessive remanent IDT can be recovered and reused.]

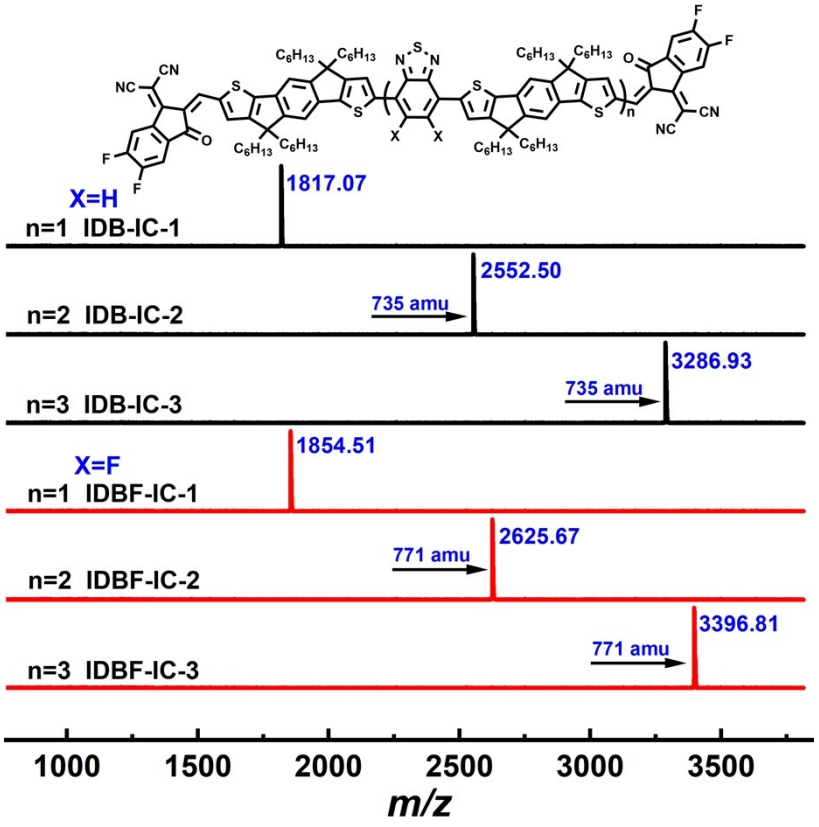

Fig. S2 Molecular ion peaks of MALDI-TOF MS spectra of IDB-IC-n and IDBF-IC-n(n=1~3)

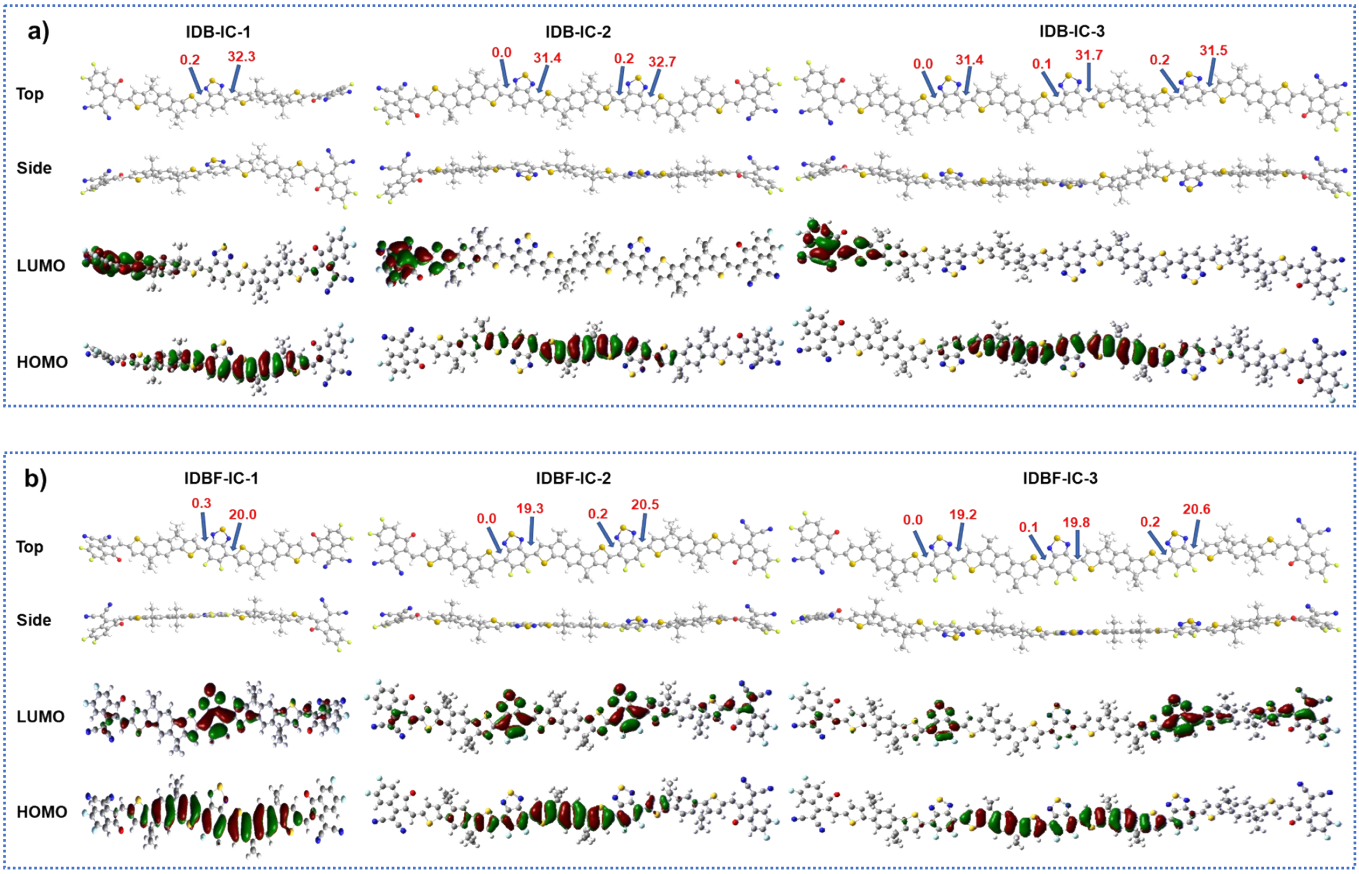

Fig. S3 Top and side views of molecular geometries and optimized geometries calculated by using density functional theory (Alkyl substituents on the IDT units of the acceptors are replaced by methyl groups for simplifying the calculation), (a) IDB-IC-n(n=1~3); (b) IDBF-IC-n(n=1~3).

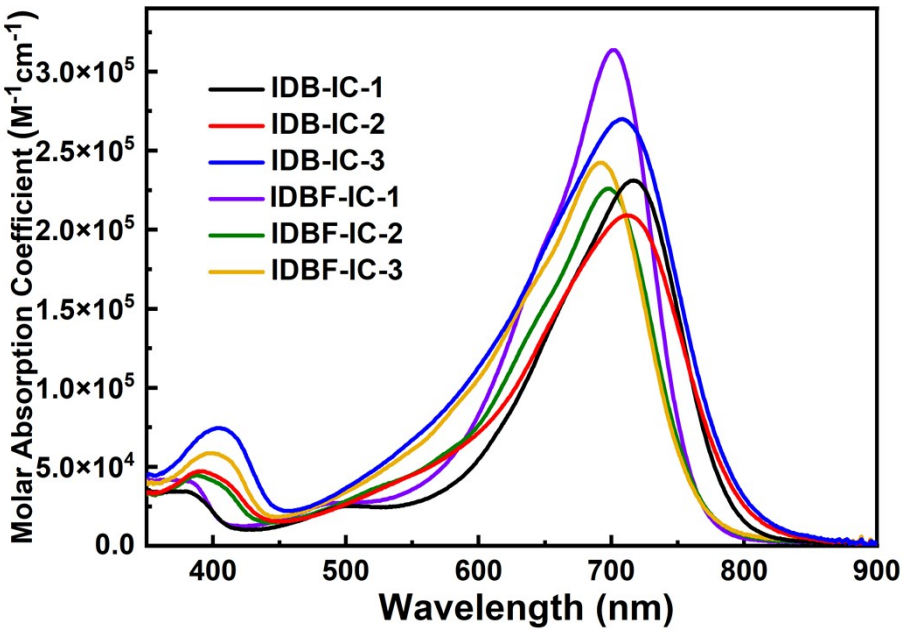

Fig. S4 UV-vis spectra of IDB(F)-IC-n(n=1~3) in chloroform solution in 10^{-6} M.

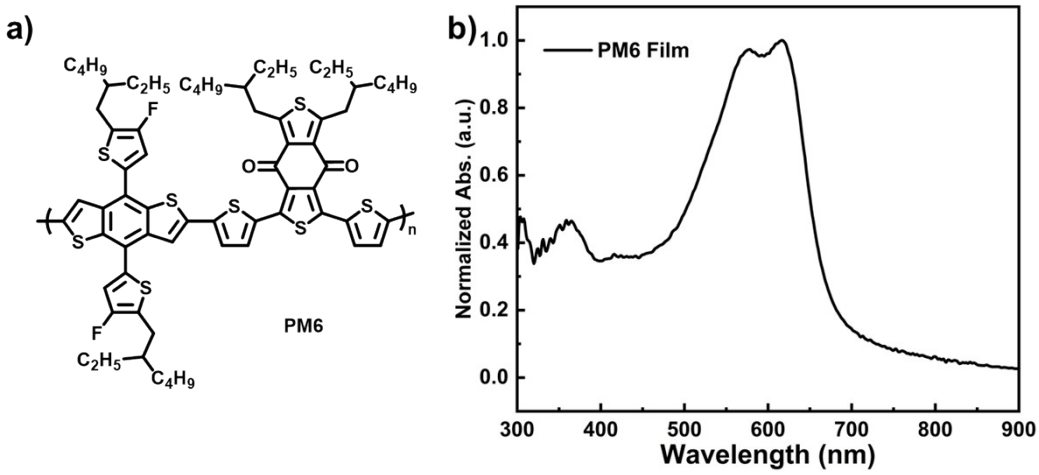

Fig. S5 Molecular structure of PM6 (a), and UV-vis absorption (c) of PM6 thin film.

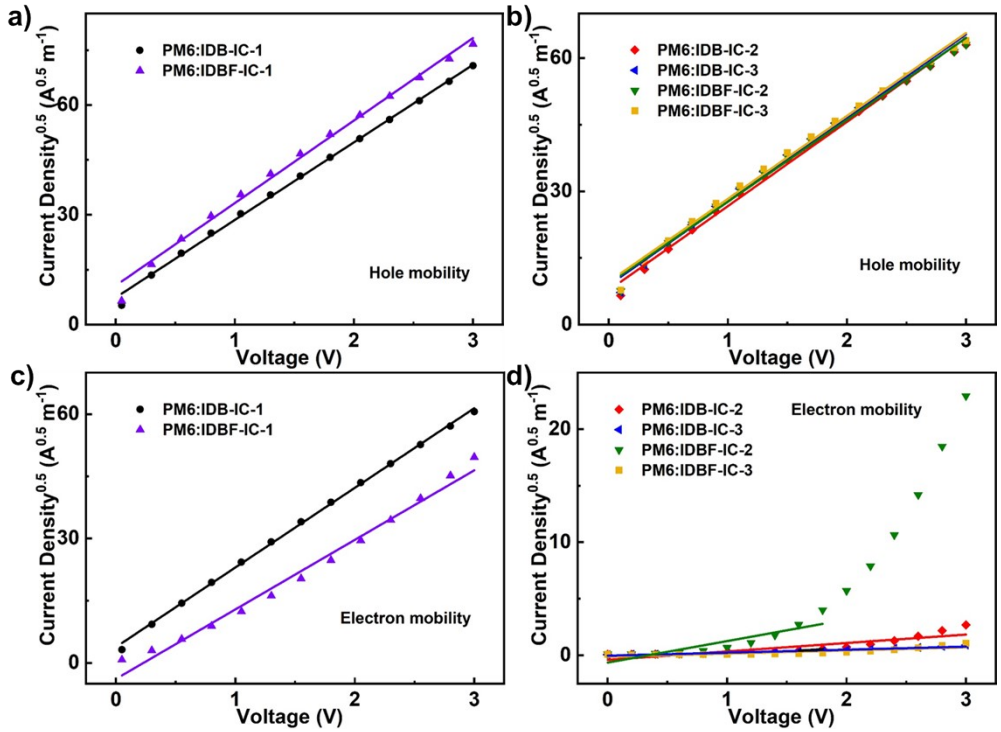

Fig. S6 (a) hole mobility measurement of IDB(F)-IC-1 optimized OPVs devices by SCLC; (b) hole mobility measurement of IDB(F)-IC-2 and 3 optimized OPVs devices by SCLC; (c) electron mobility measurement of IDB(F)-IC-1 optimized OPVs devices by SCLC; (d) electron mobility measurement of IDB(F)-IC-2 and 3 optimized OPVs devices by SCLC.

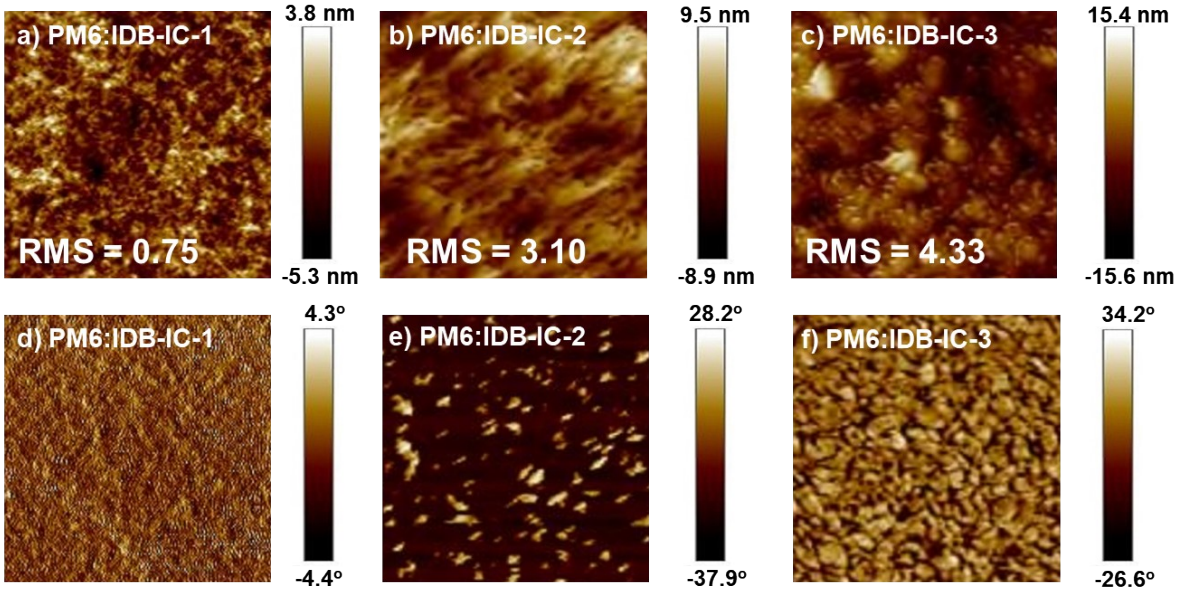

Fig. S7 AFM height (a, b, c) and phase (d, e, f) images of blends PM6:IDB-IC-n(n=1~3).

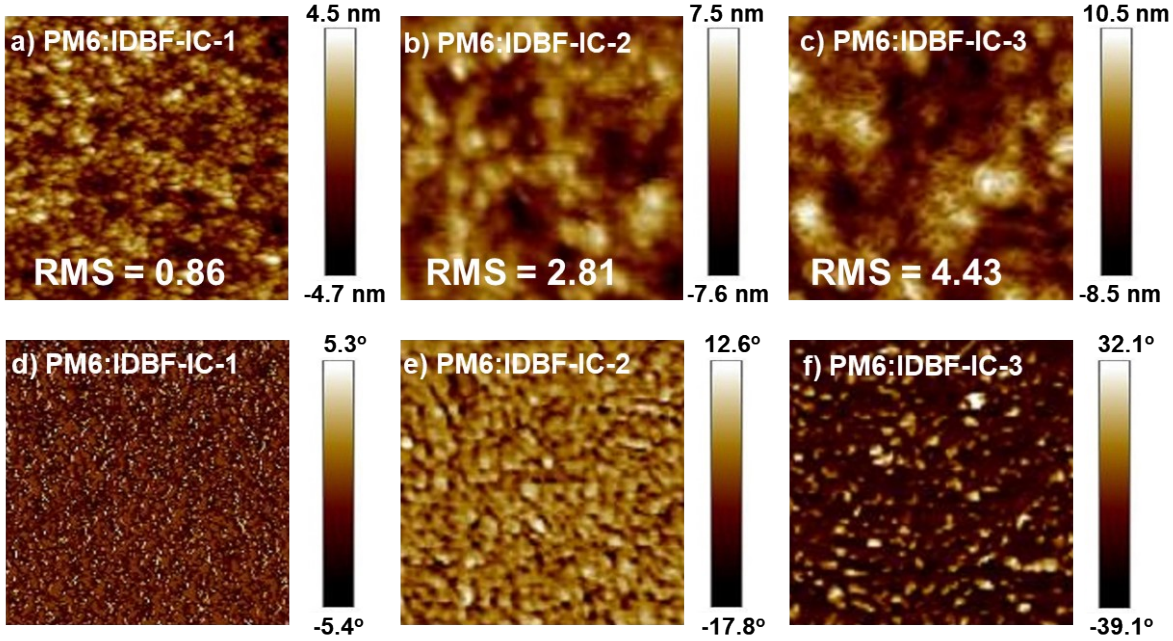

Fig. S8 AFM height (a, b, c) and phase (d, e, f) images of blends PM6:IDBF-IC-n(n=1~3).

Table S1 Photovoltaic parameters of OSCs based on PM6:IDB-IC-1 blended films under the illumination of AM 1.5 G, 100 mW cm^{-2}.

PM6:IDB-IC-1	V_{oc} V	J_{sc} mA cm^{-2}	FF %	PCE %
1:1 (w/o)	0.905	12.78	63.36	7.36
1:1 (TA)	0.900	14.32	68.46	8.86
1:1.2 (w/o)	0.901	15.09	66.37	9.11
1:1.2 (TA)	**0.892**	**16.13 (15.53)**	**71.02**	**10.32**
1:1.2 (0.5% DIO + TA)	0.872	16.03	69.35	9.79
1:1.2 (0.5% CN + TA)	0.878	15.74	68.94	9.56
1:1.4 (w/o)	0.892	15.18	63.68	8.66
1:1.4 (TA)	0.884	15.66	64.29	8.96

Table. S2. Photovoltaic parameters of OSCs based on PM6:IDBF-IC-1 blended films under the illumination of AM 1.5 G, 100 mW cm^{-2}

PM6:IDBF-IC-1	V_{oc} V	J_{sc} mA cm^{-2}	FF %	PCE %
1.2:1 (w/o)	0.894	18.02	64.16	10.37
1.2:1 (TA)	0.893	18.69	64.58	10.81
1:1 (w/o)	0.905	18.25	66.00	11.13
1:1 (TA)	**0.901**	**19.17(18.58)**	**69.50**	**12.12**
1:1 (0.5% DIO + TA)	0.886	19.45	66.61	11.51
1:1 (0.5% CN + TA)	0.883	17.65	61.24	9.57
1:1.2 (w/o)	0.920	18.14	66.62	11.23
1:1.2 (TA)	0.894	18.97	71.02	11.44
1:1.4 (w/o)	0.920	16.94	68.52	10.79
1:1.4 (TA)	0.901	17.42	69.40	11.00

Table S3 Hole and electron mobilities of PDFCs measured in single carrier diodes by fitting of SCLC model.

Blends	μ_h (10^{-4} cm^2 V^{-1} s^{-1})	μ_e(10^{-4} cm^2 V^{-1} s^{-1})
PM6:IDB-IC-1	1.51	1.23
PM6:IDB-IC-2	1.20	0.00188
PM6:IDB-IC-3	1.19	0.000244
PM6:IDBF-IC-1	1.70	0.94
PM6:IDBF-IC-2	1.14	0.0121
PM6:IDBF-IC-3	1.17	0.000262

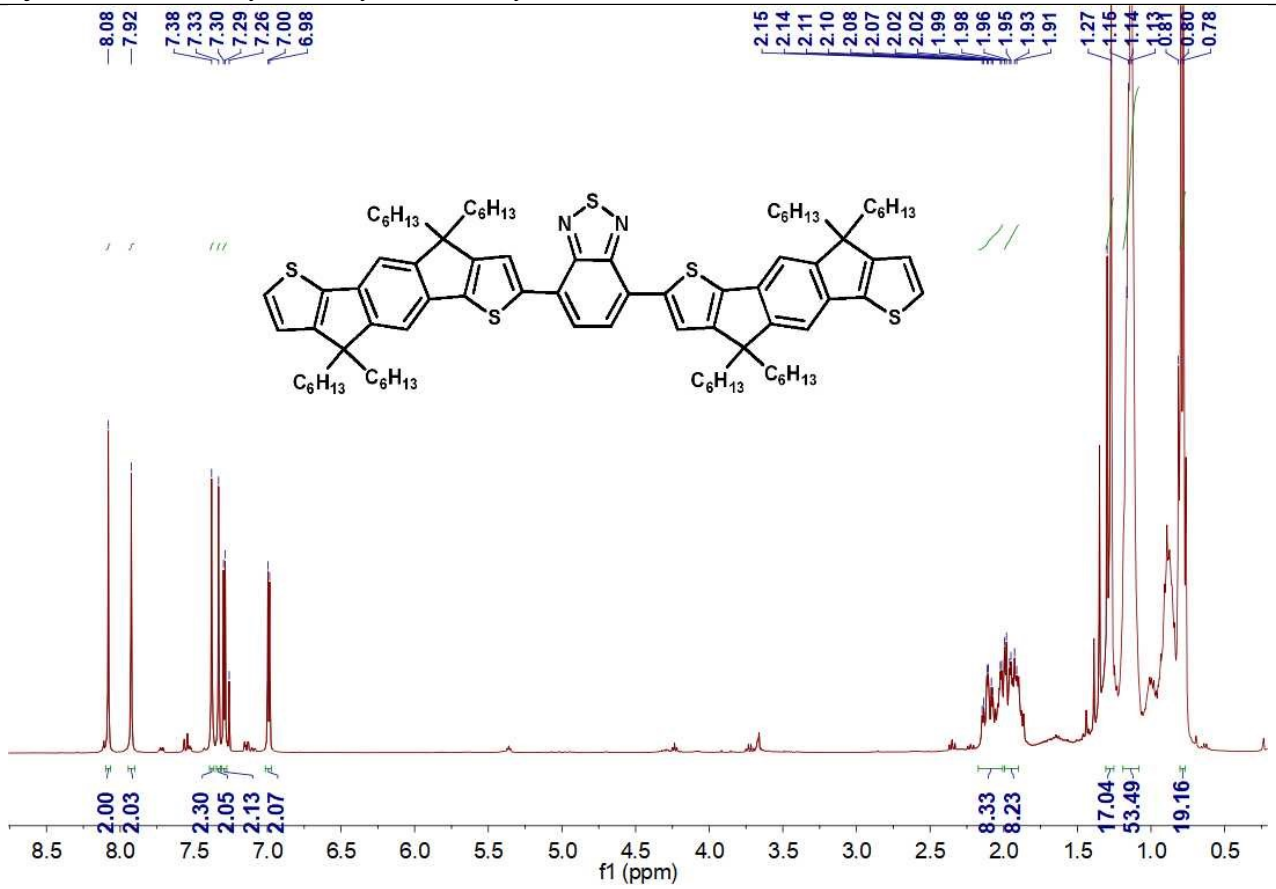

Fig. S9 ^{1}H NMR spectra of alt-(IDT-BT)-1 in $CDCl_3$.

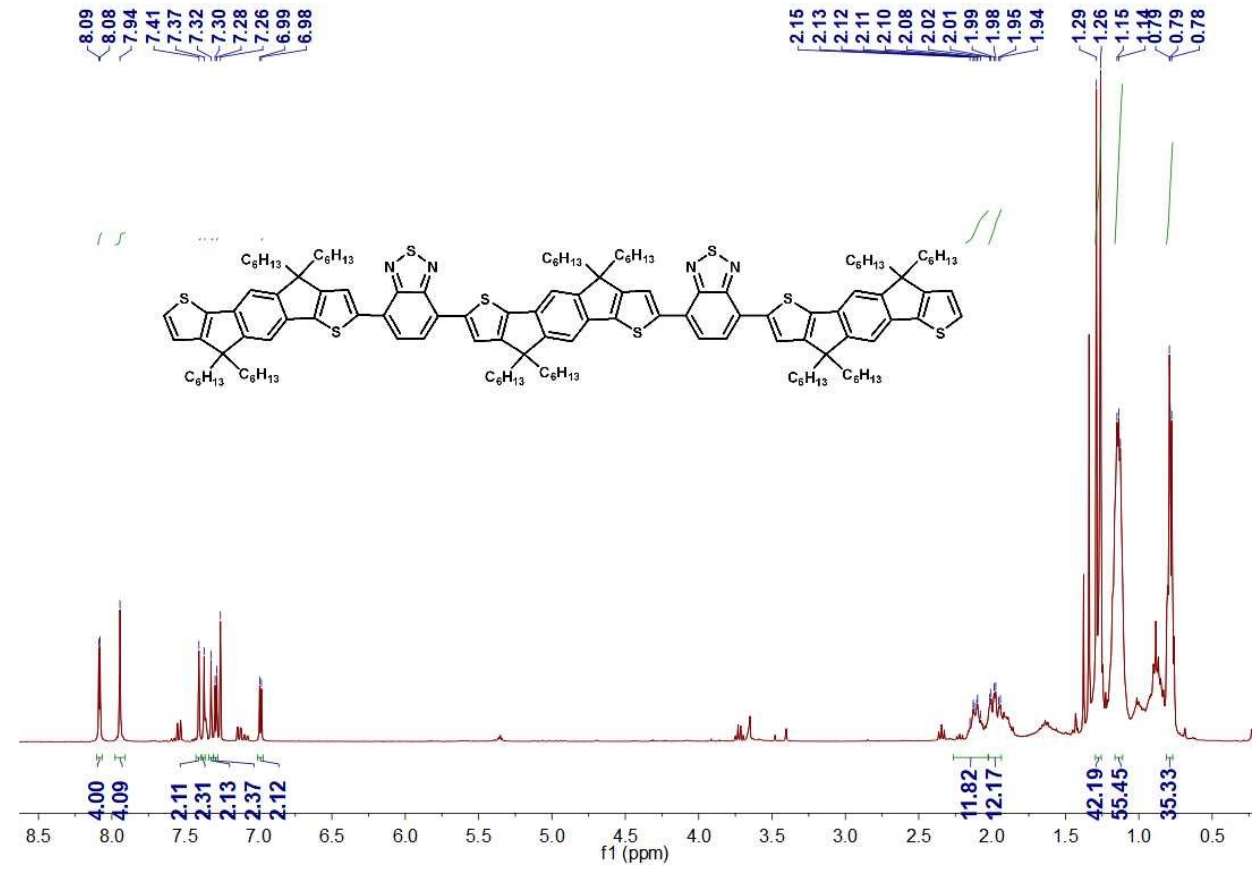

Fig. S10 ^{1}H NMR spectra of alt-(IDT-BT)-2 in $CDCl_3$.

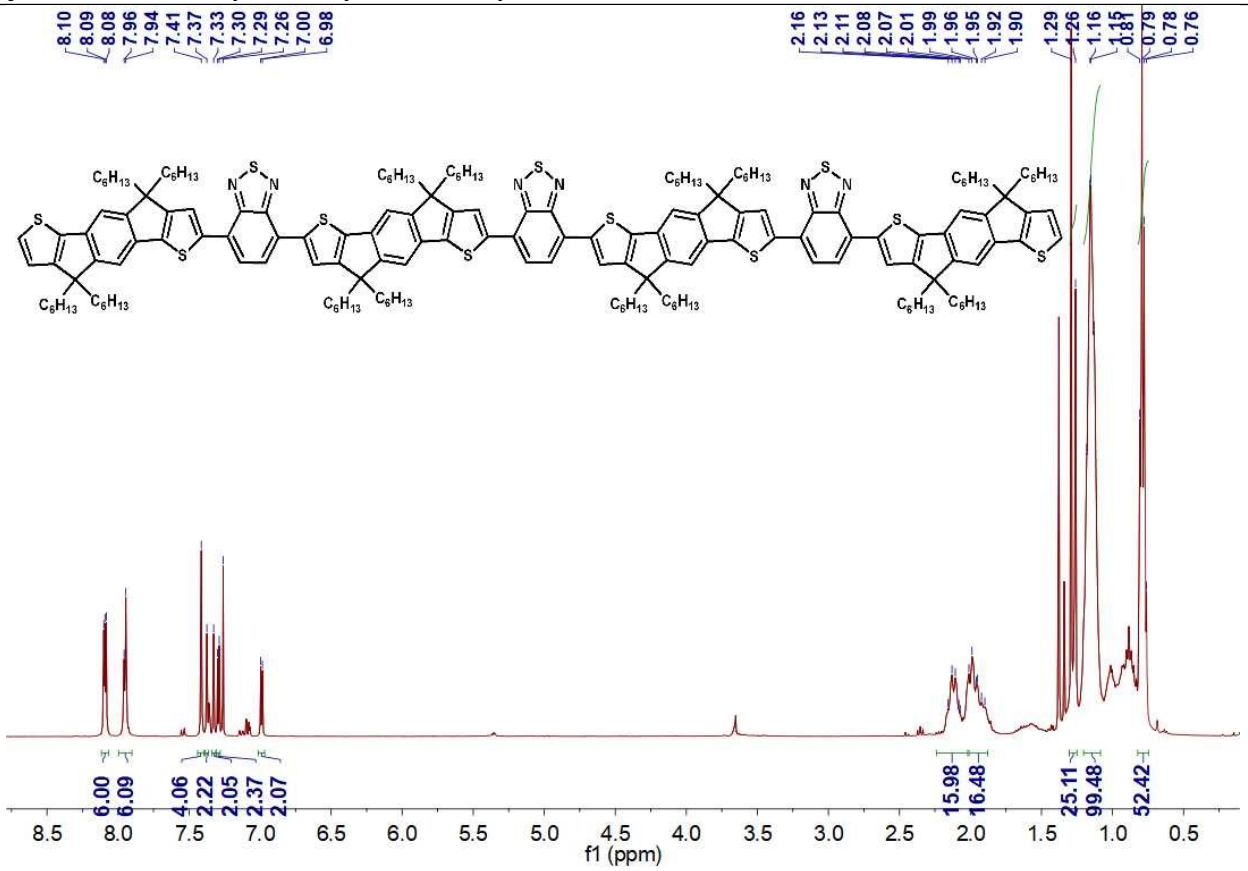

Fig. S11 ^{1}H NMR spectra of alt-(IDT-BT)-3 in $CDCl_3$.

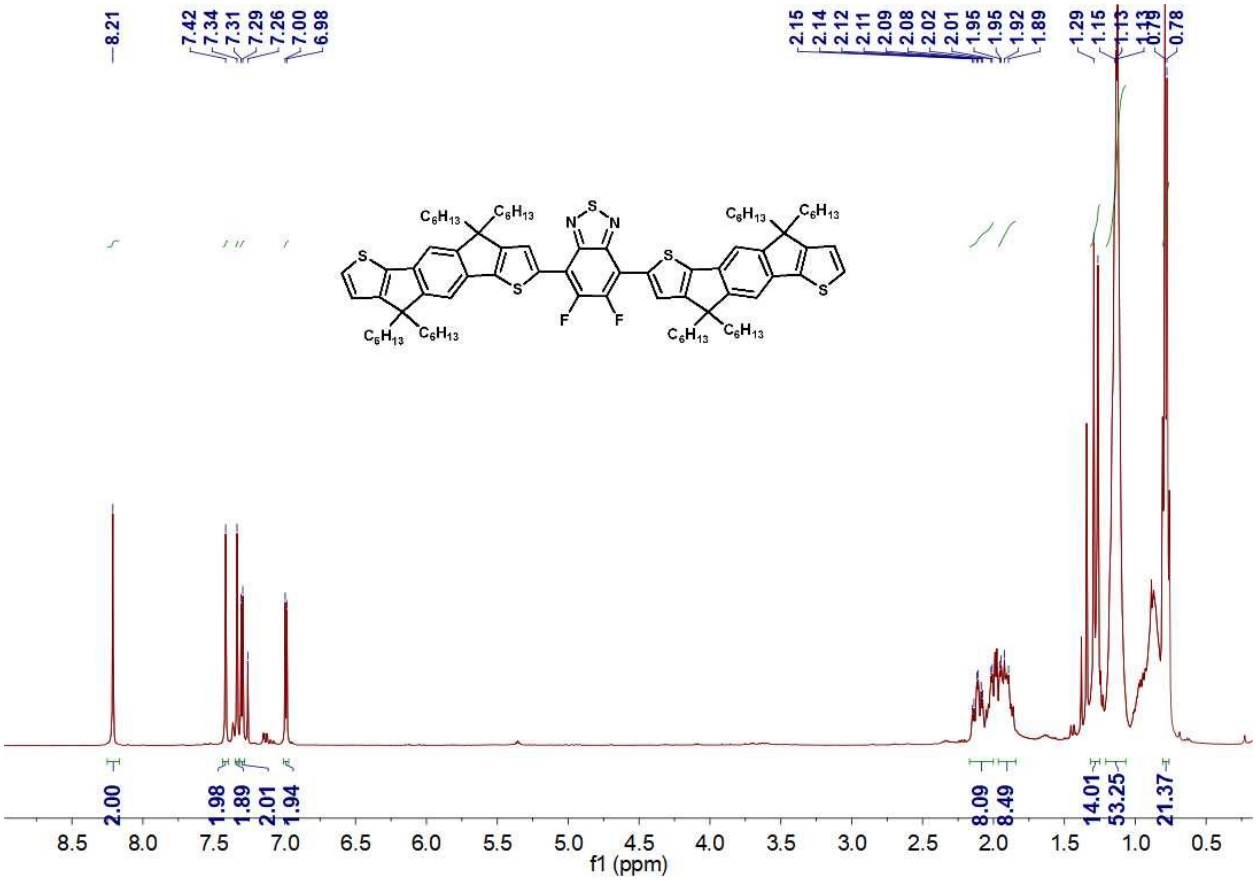

Fig. S12 ^{1}H NMR spectra of alt-(IDT-DFBT)-1 in $CDCl_3$.

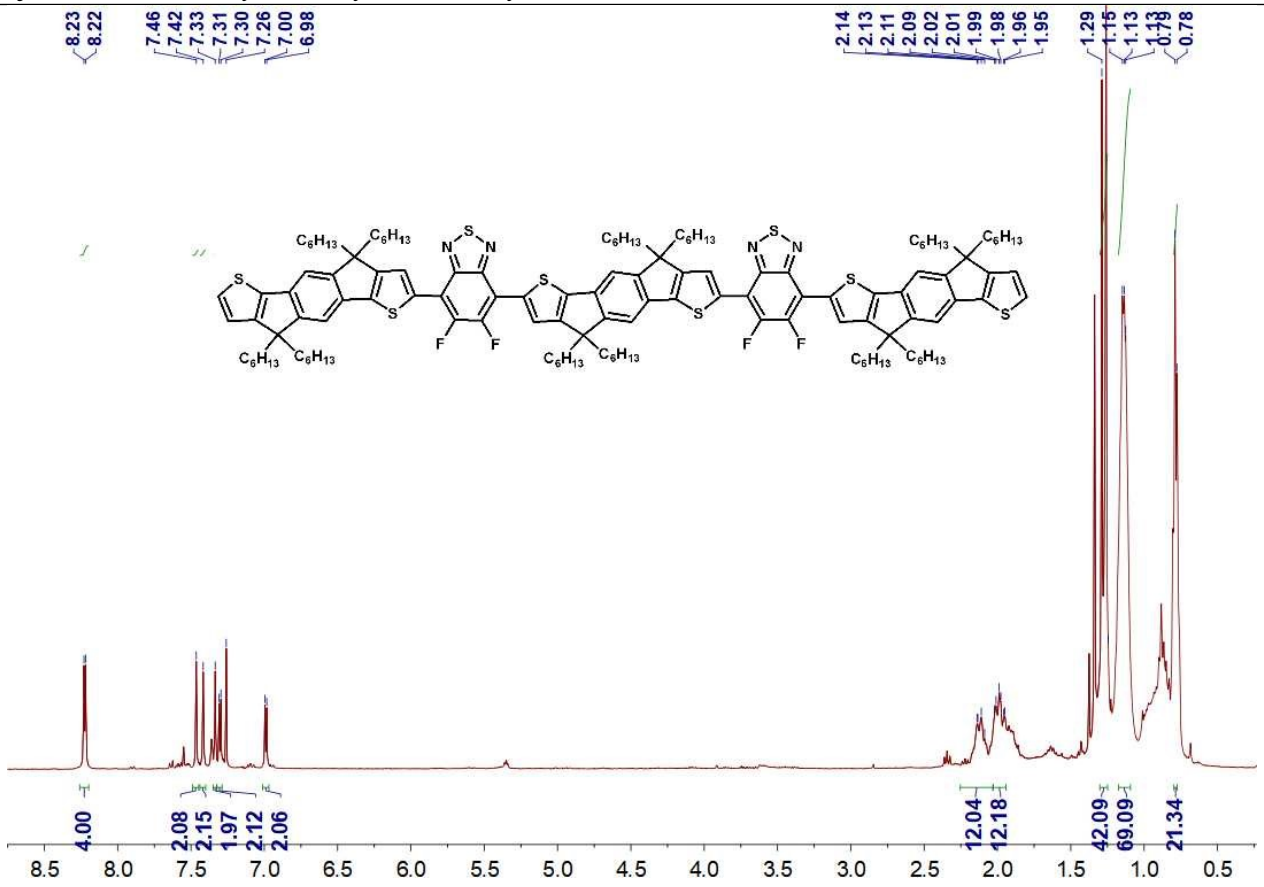

Fig. S13 ^{1}H NMR spectra of alt-(IDT-DFBT)-2 in $CDCl_3$.

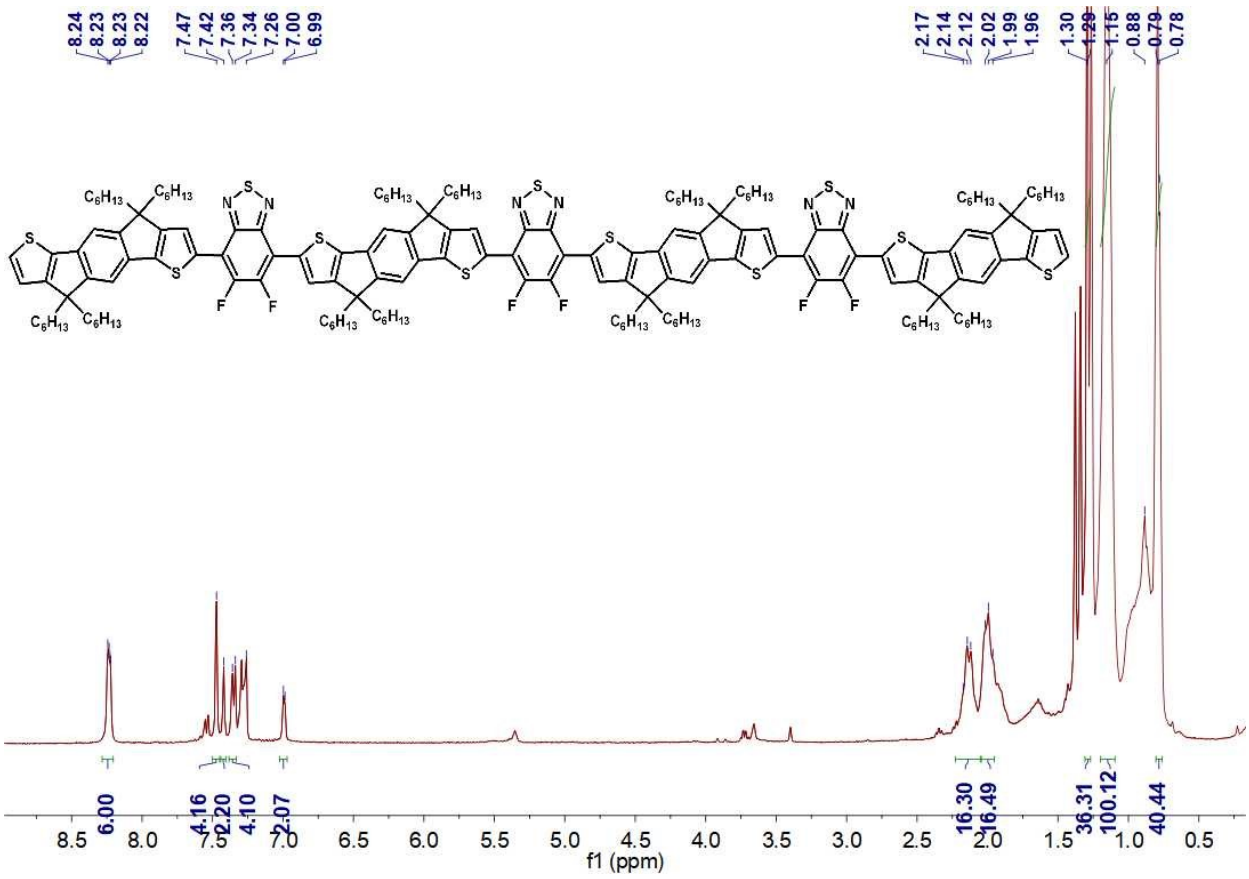

Fig. S14 ^{1}H NMR spectra of alt-(IDT-DFBT)-3 in $CDCl_3$.

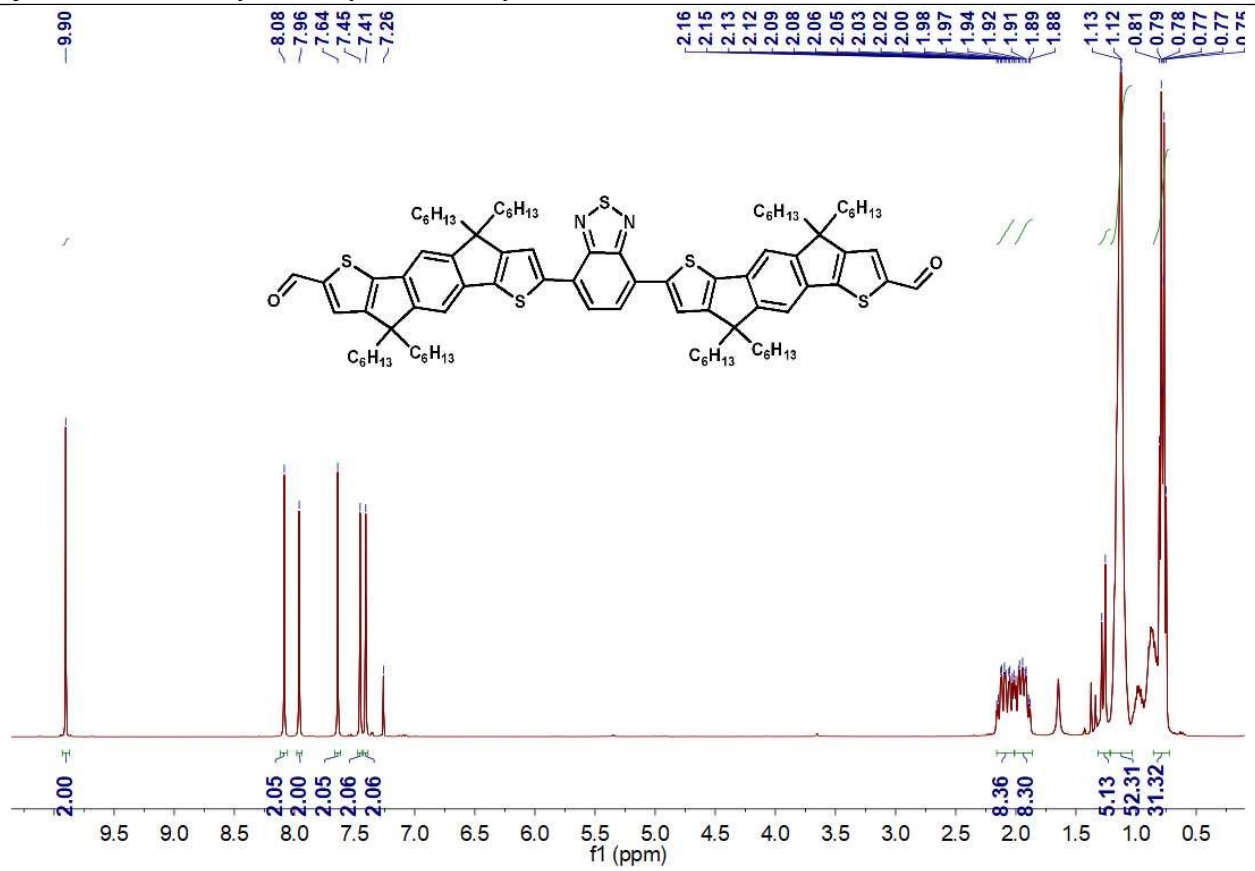

Fig. S15 ^{1}H NMR spectra of aldehyde intermediate1a in $CDCl_3$.

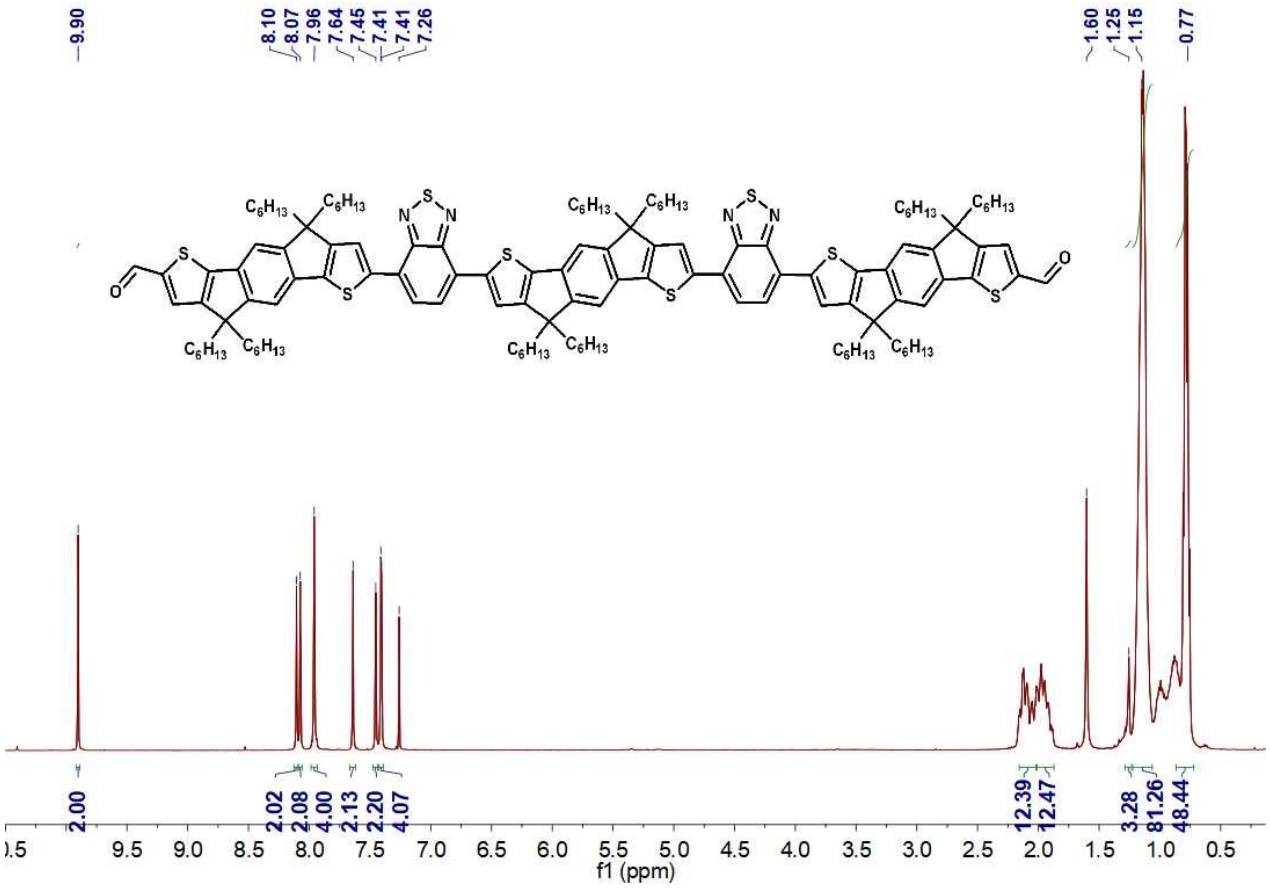

Fig. S16 ^{1}H NMR spectra of aldehyde intermediate1b in $CDCl_3$.

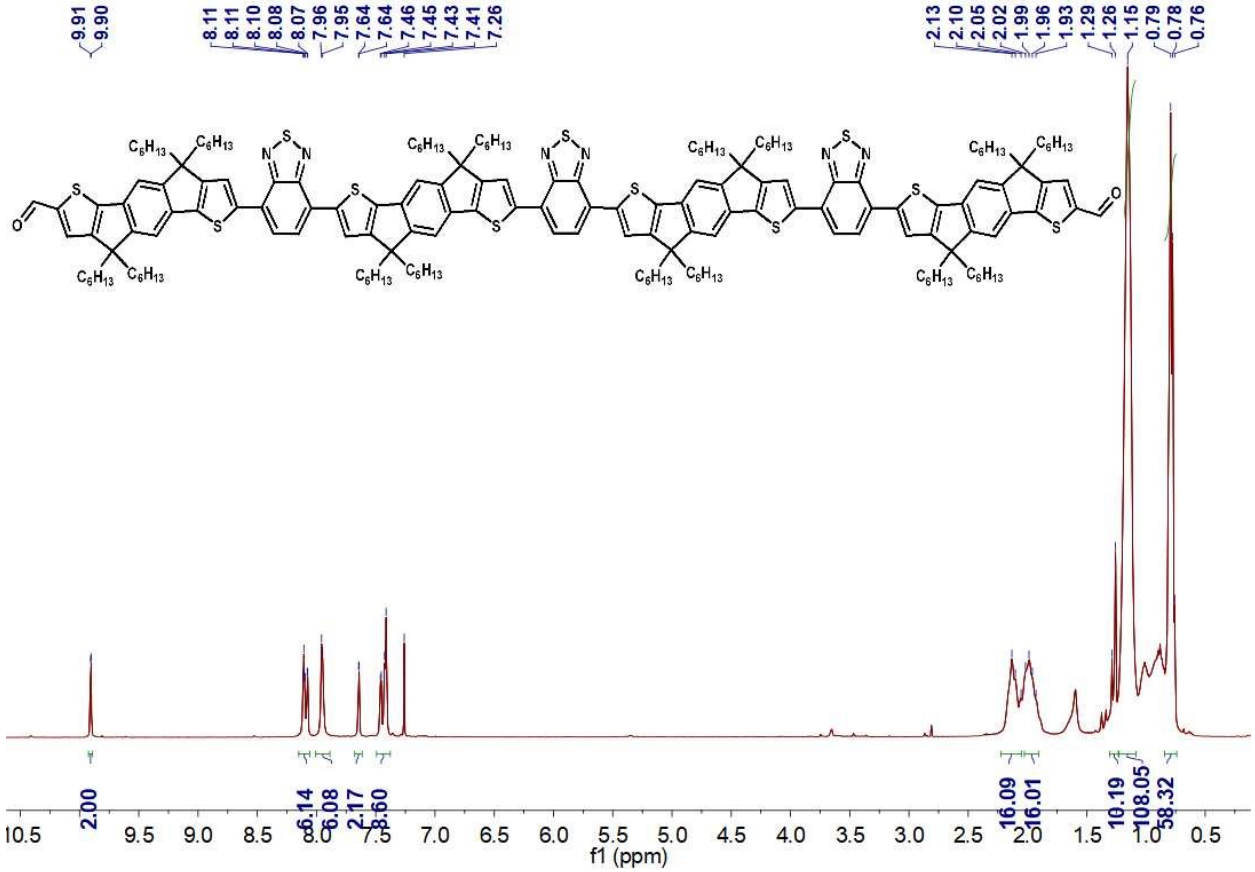

Fig. S17 ^{1}H NMR spectra of aldehyde intermediate1c in $CDCl_3$.

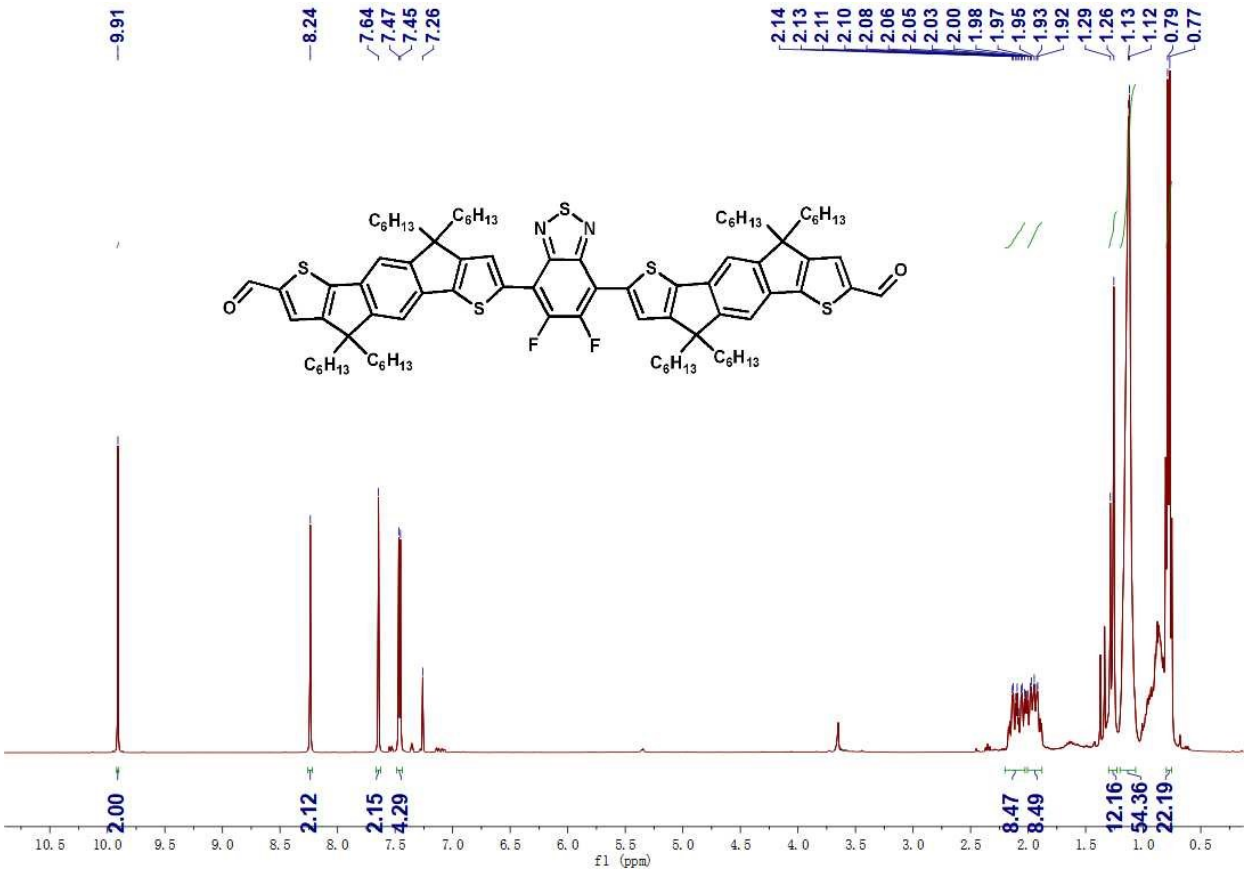

Fig. S18 ^{1}H NMR spectra of aldehyde intermediate 2a in $CDCl_3$.

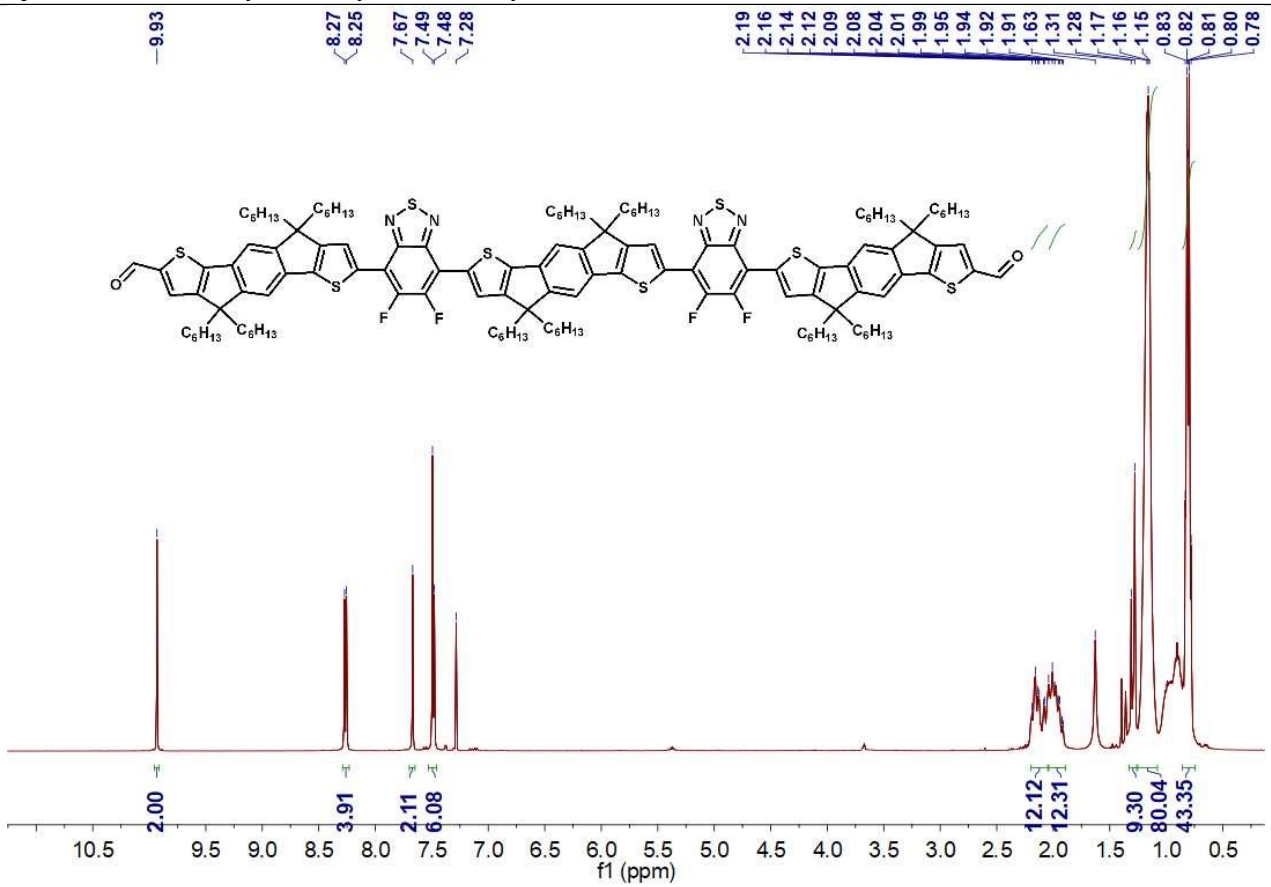

Fig. S19 ^{1}H NMR spectra of aldehyde intermediate 2b in $CDCl_3$.

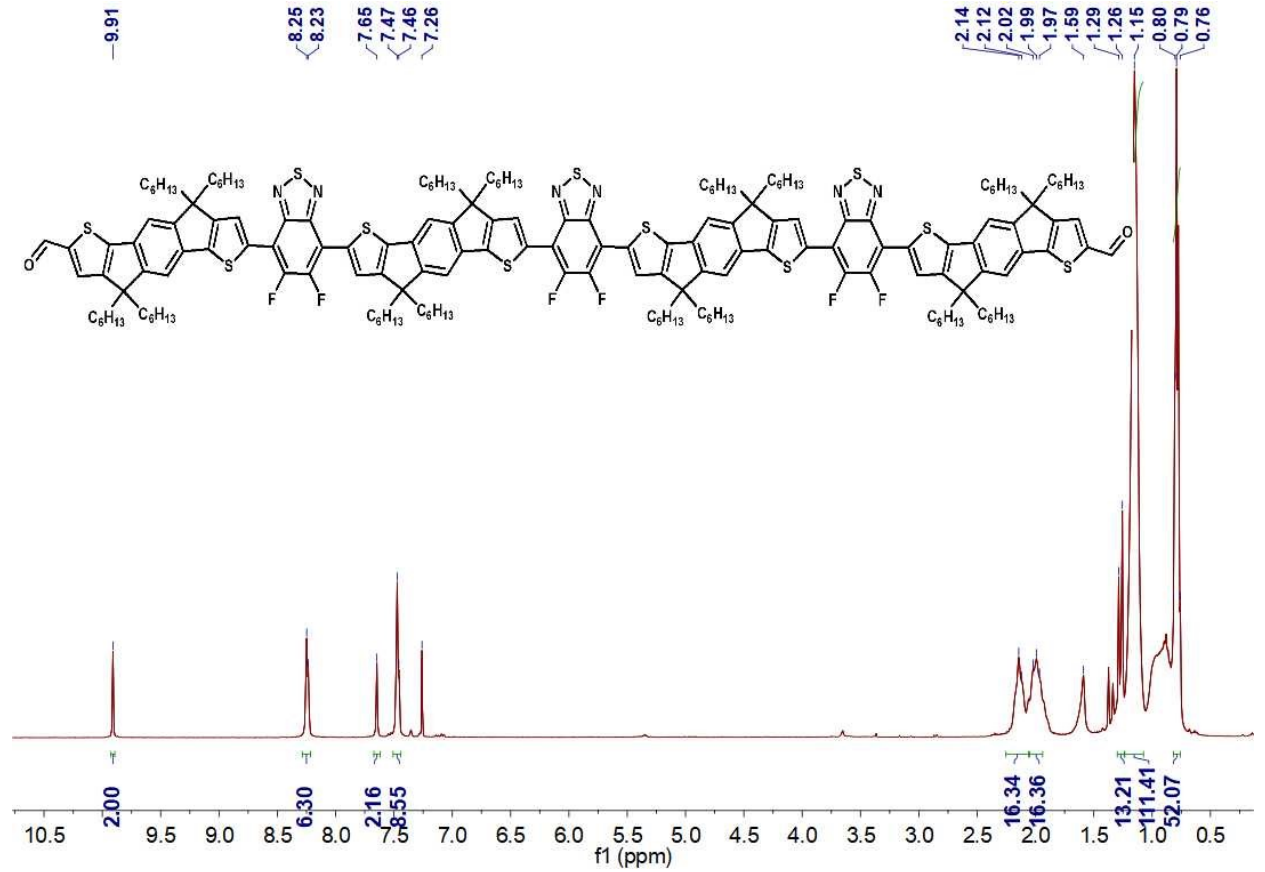

Fig. S20 ^{1}H NMR spectra of aldehyde intermediate 2c in $CDCl_3$.

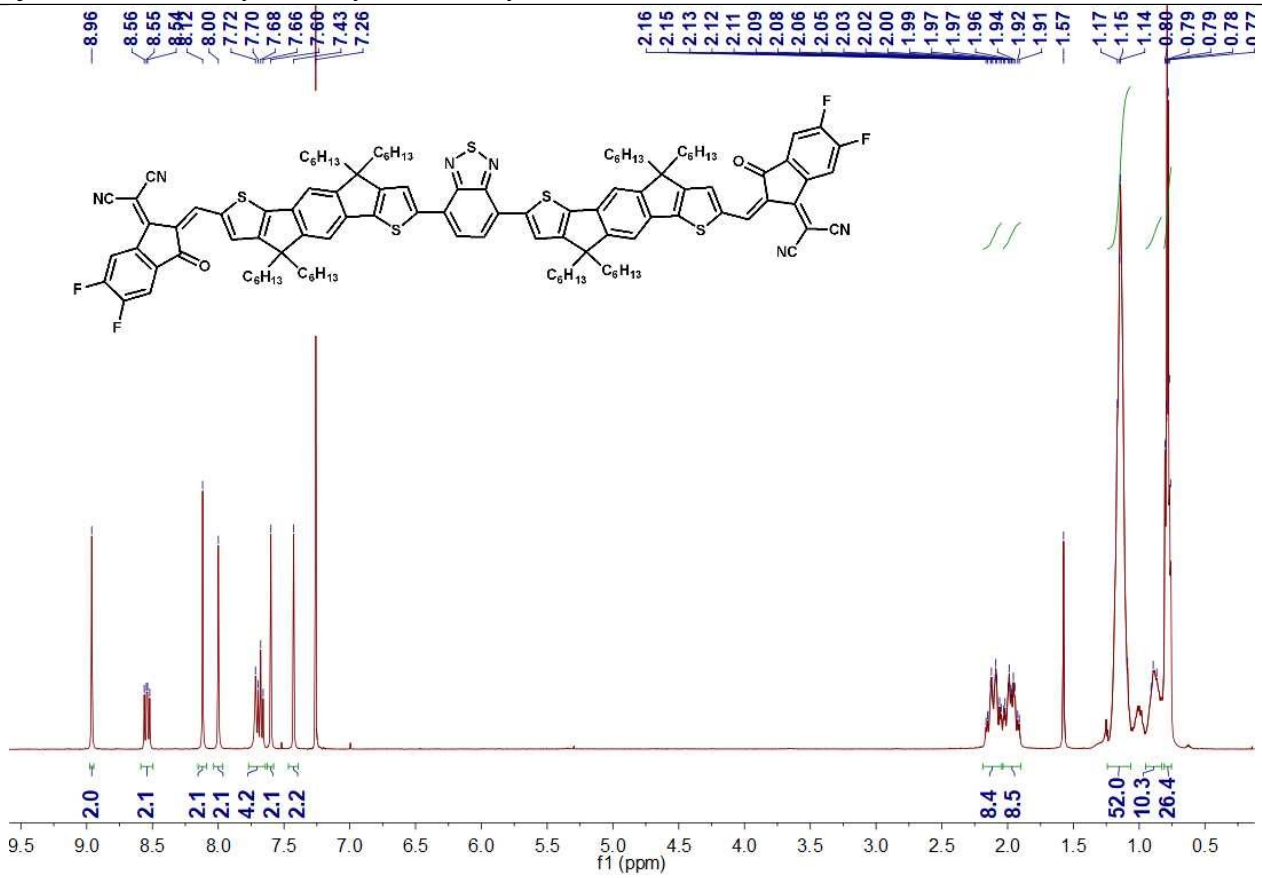

Fig. S21 ^{1}H NMR spectra of IDB-IC-1in $CDCl_3$.

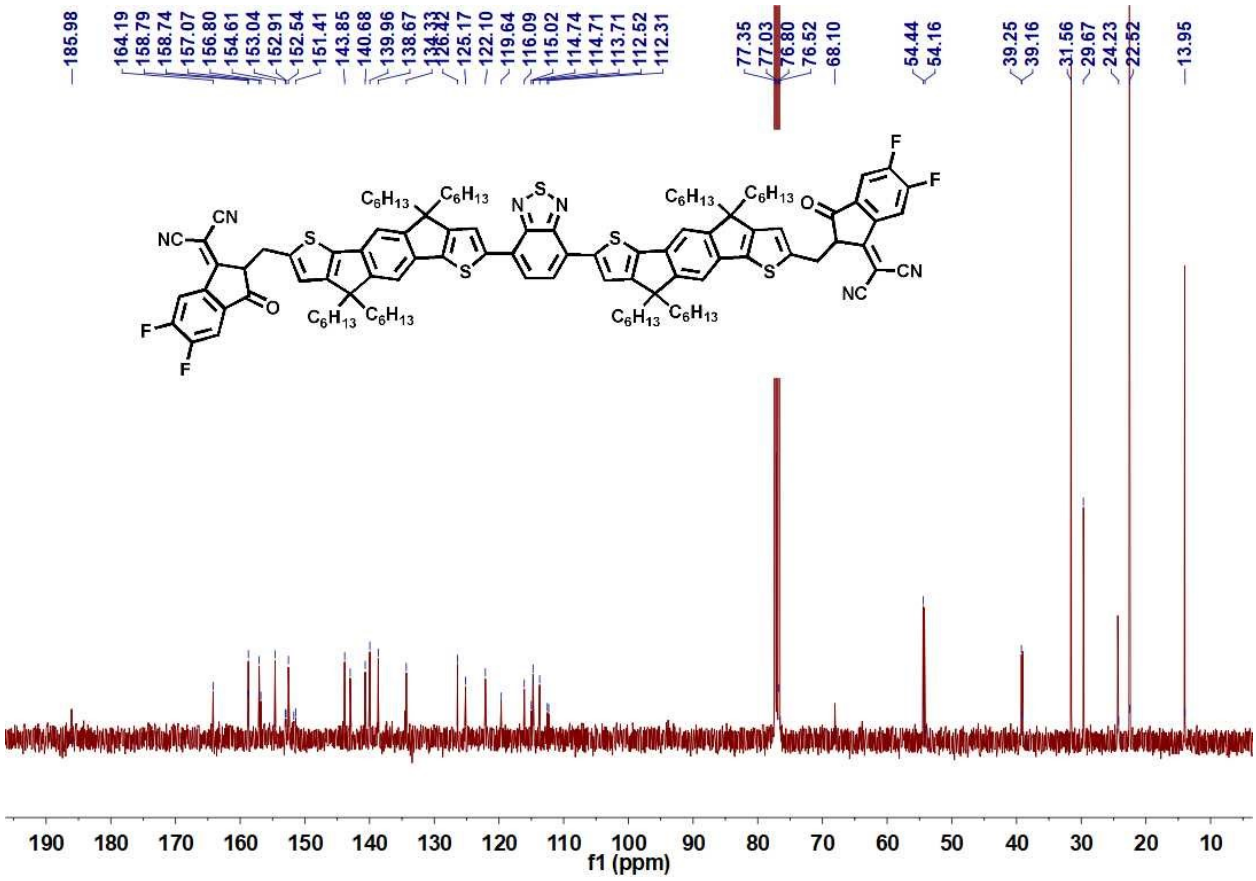

Fig. S22 ^{13}C NMR spectra of IDB-IC-1in $CDCl_3$.

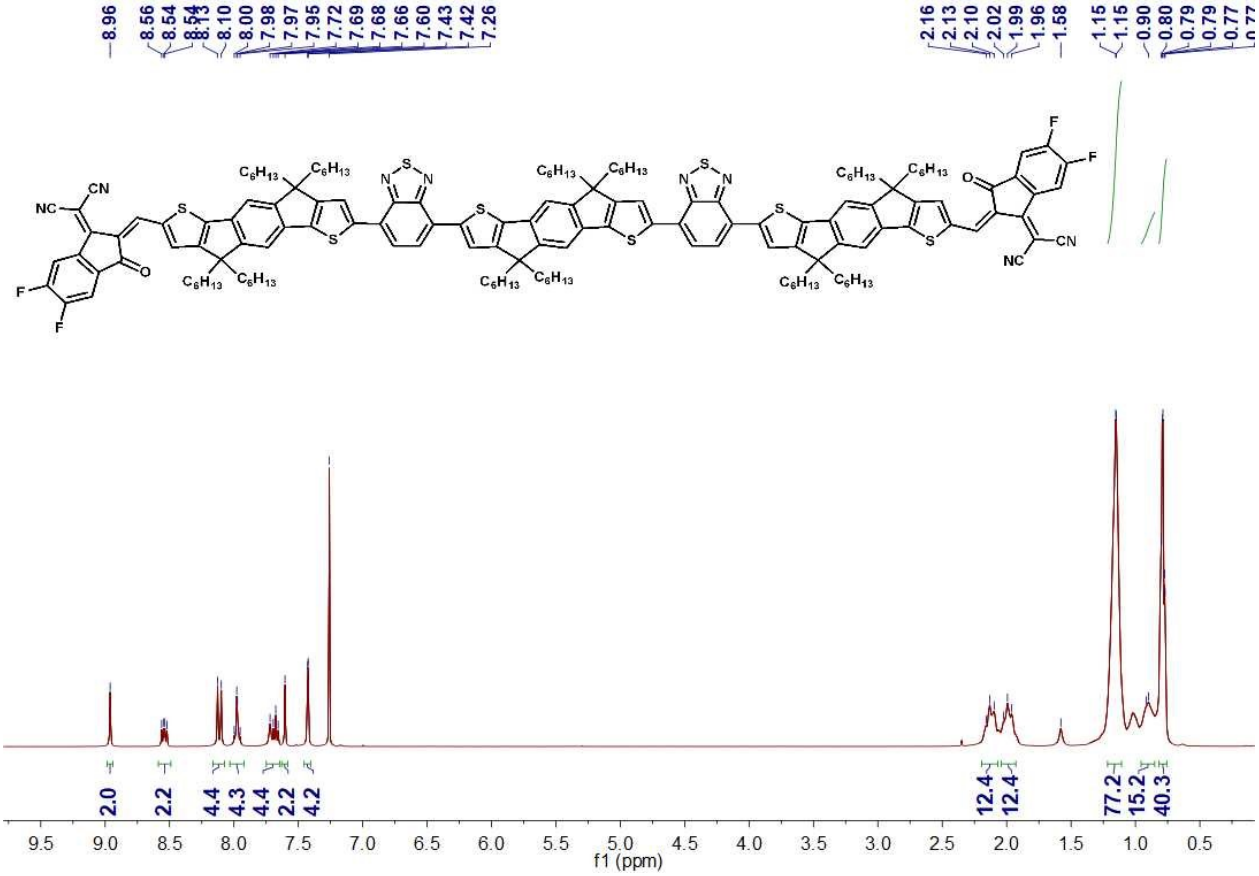

Fig. S23 ^{1}H NMR spectra of IDB-IC-2 in $CDCl_3$.

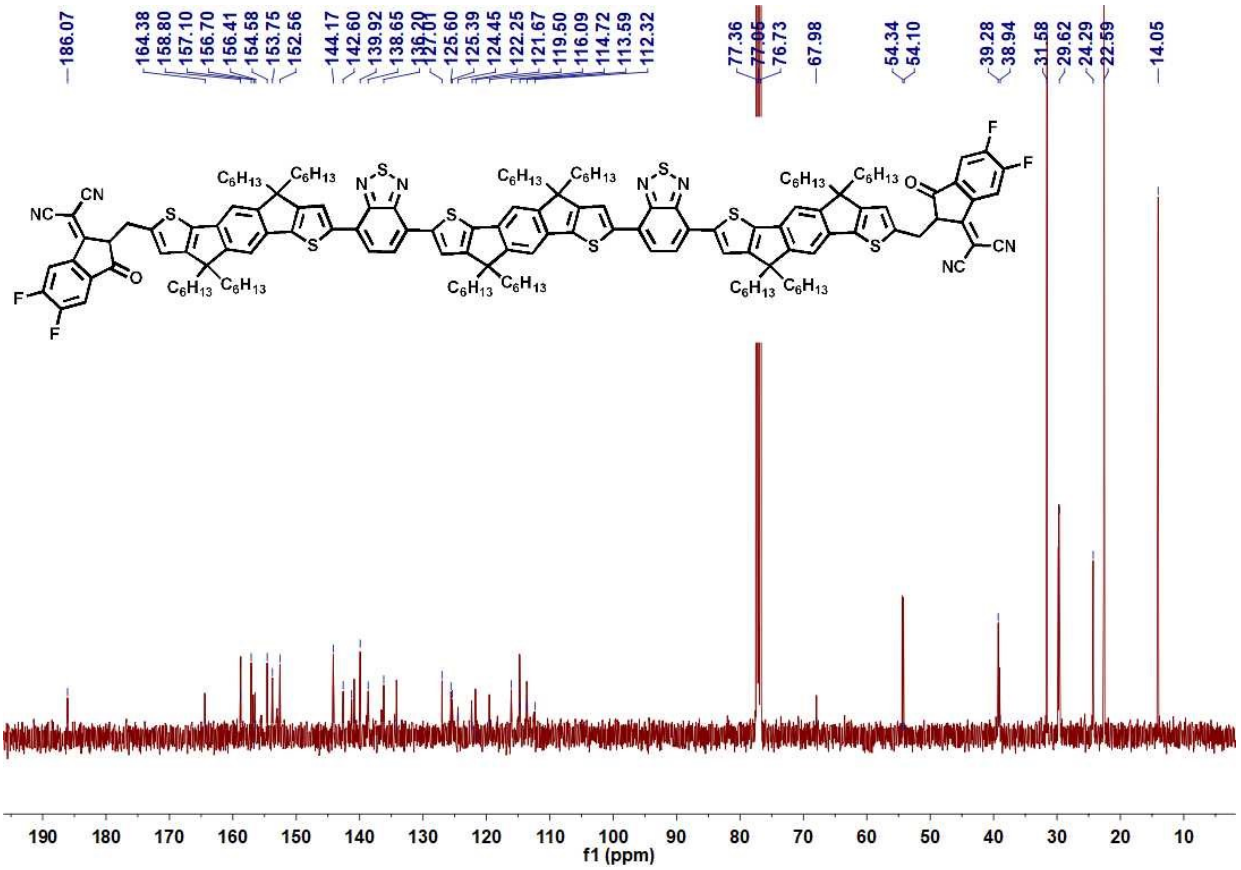

Fig. S24 ^{13}C NMR spectra of IDB-IC-2 in $CDCl_3$.

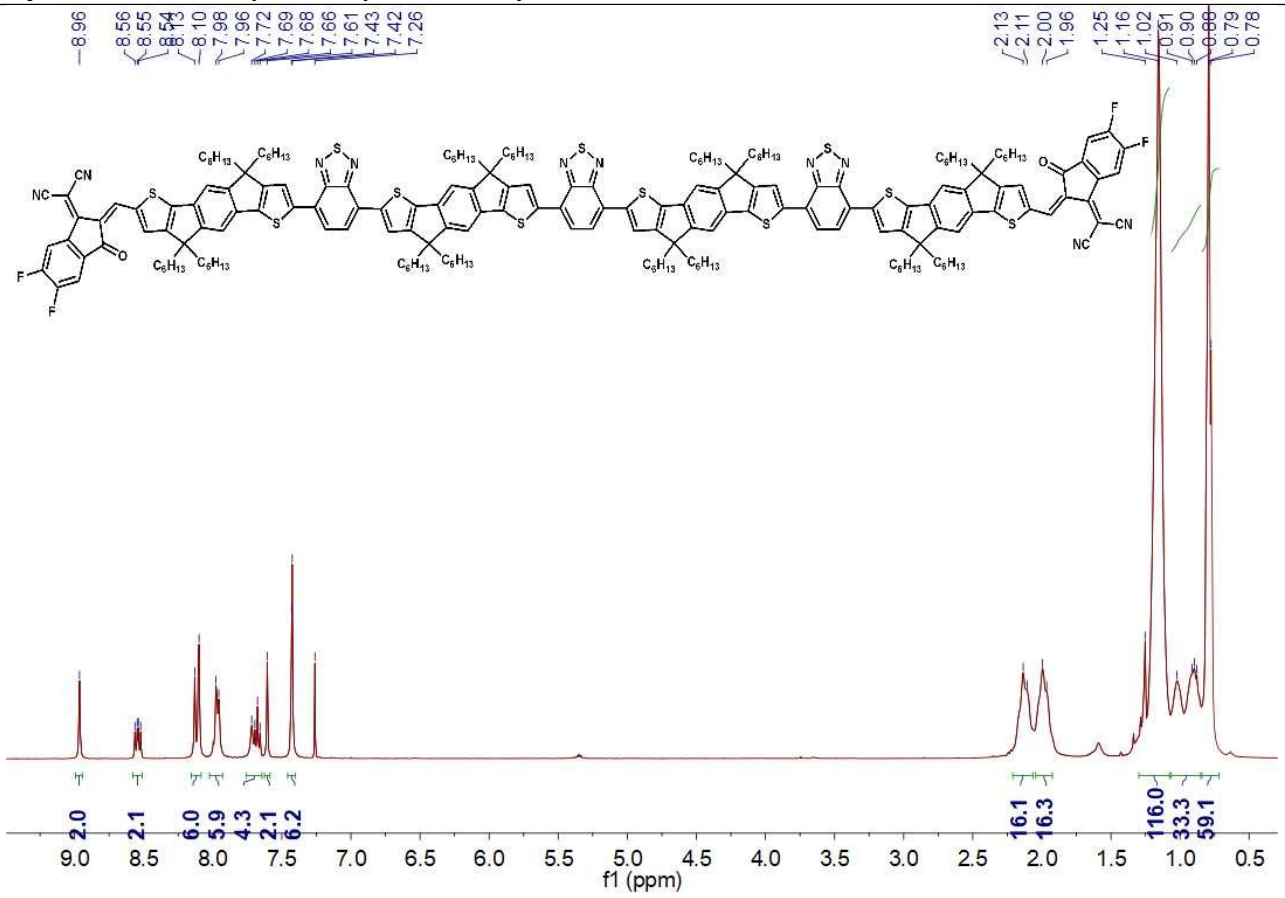

Fig. S25 ^{1}H NMR spectra of IDB-IC-3 in $CDCl_3$.

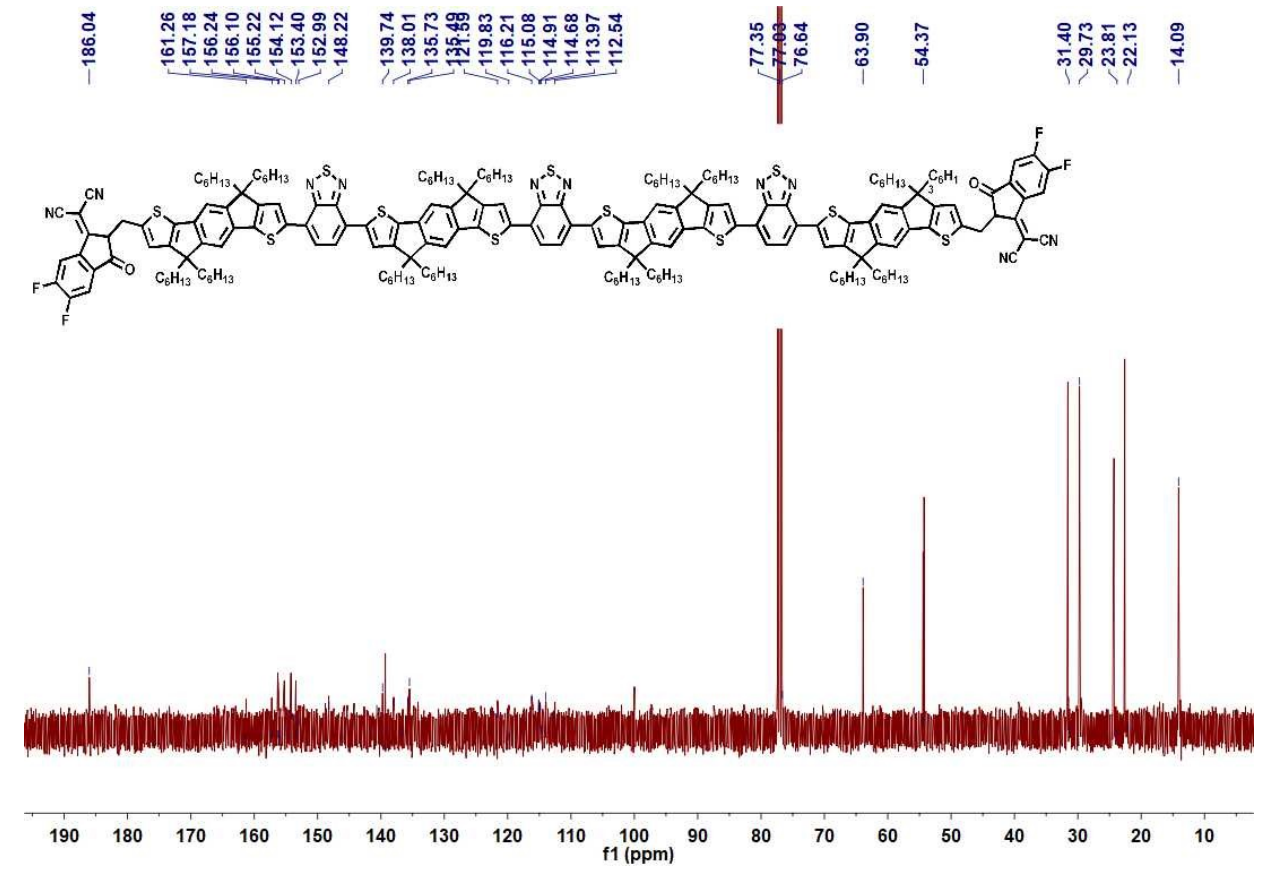

Fig. S26 ^{13}C NMR spectra of IDB-IC-3 in $CDCl_3$.

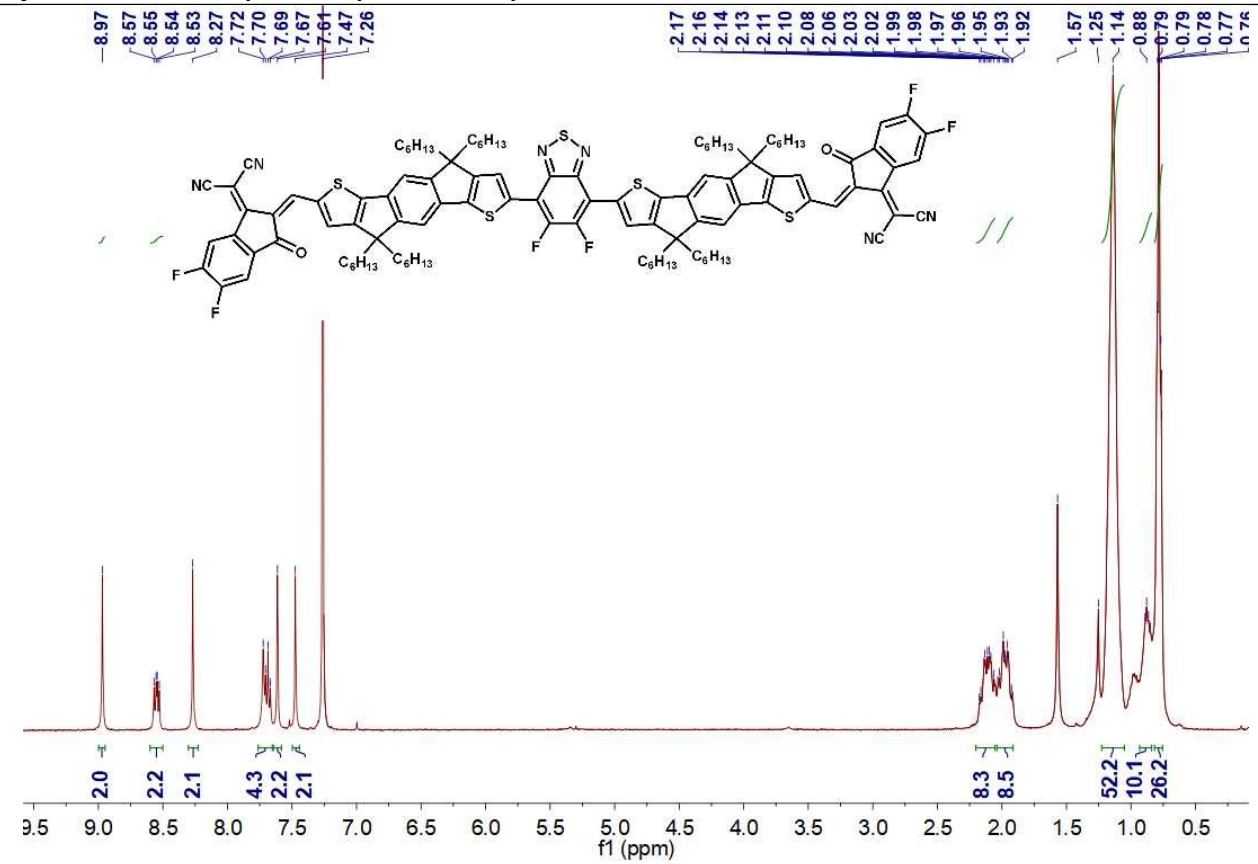

Fig. S27 ^{1}H NMR spectra of IDBF-IC-1in $CDCl_3$.

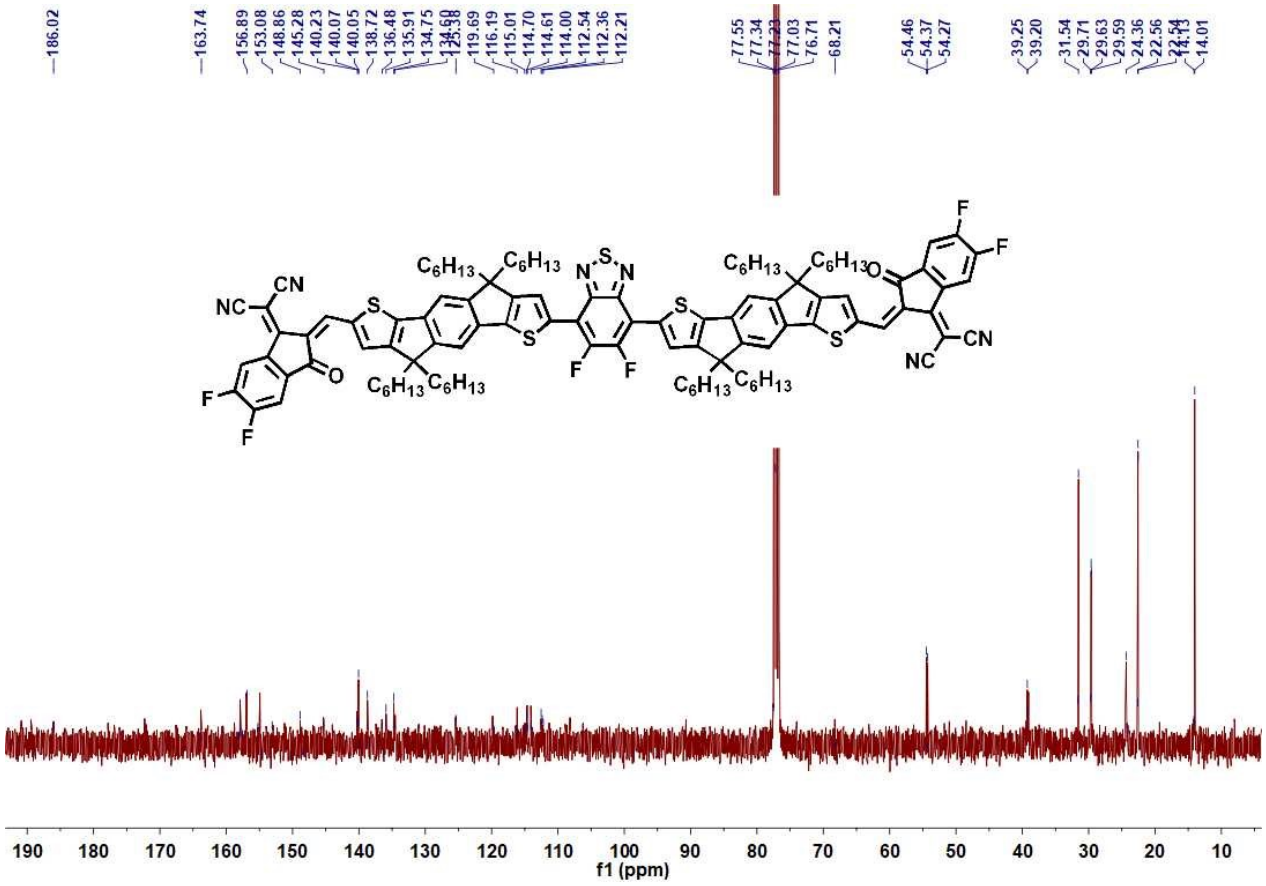

Fig. S28 ^{13}C NMR spectra of IDBF-IC-1in $CDCl_3$.

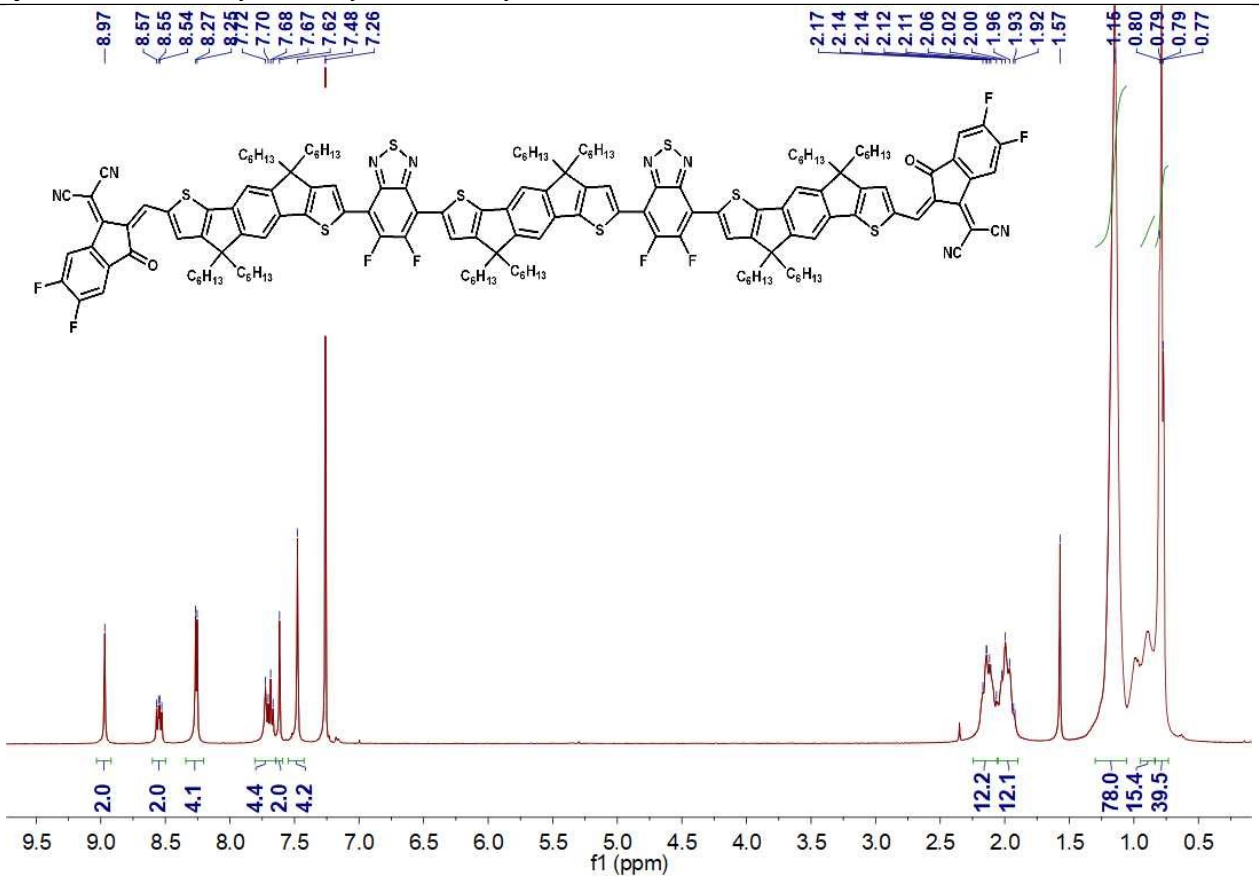

Fig. S29 ^{1}H NMR spectra of IDBF-IC-2 in $CDCl_3$.

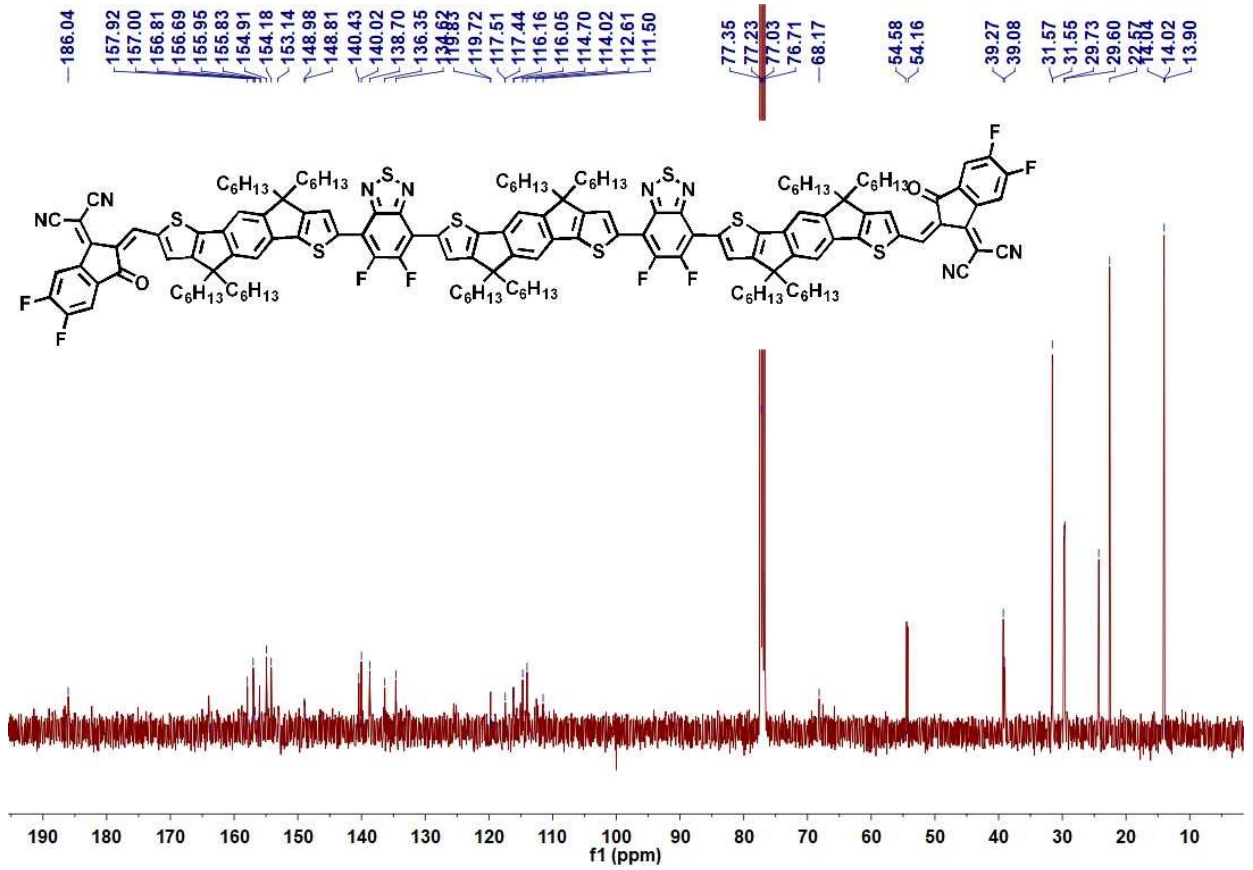

Fig. S30 ^{13}C NMR spectra of IDBF-IC-2 in $CDCl_3$.

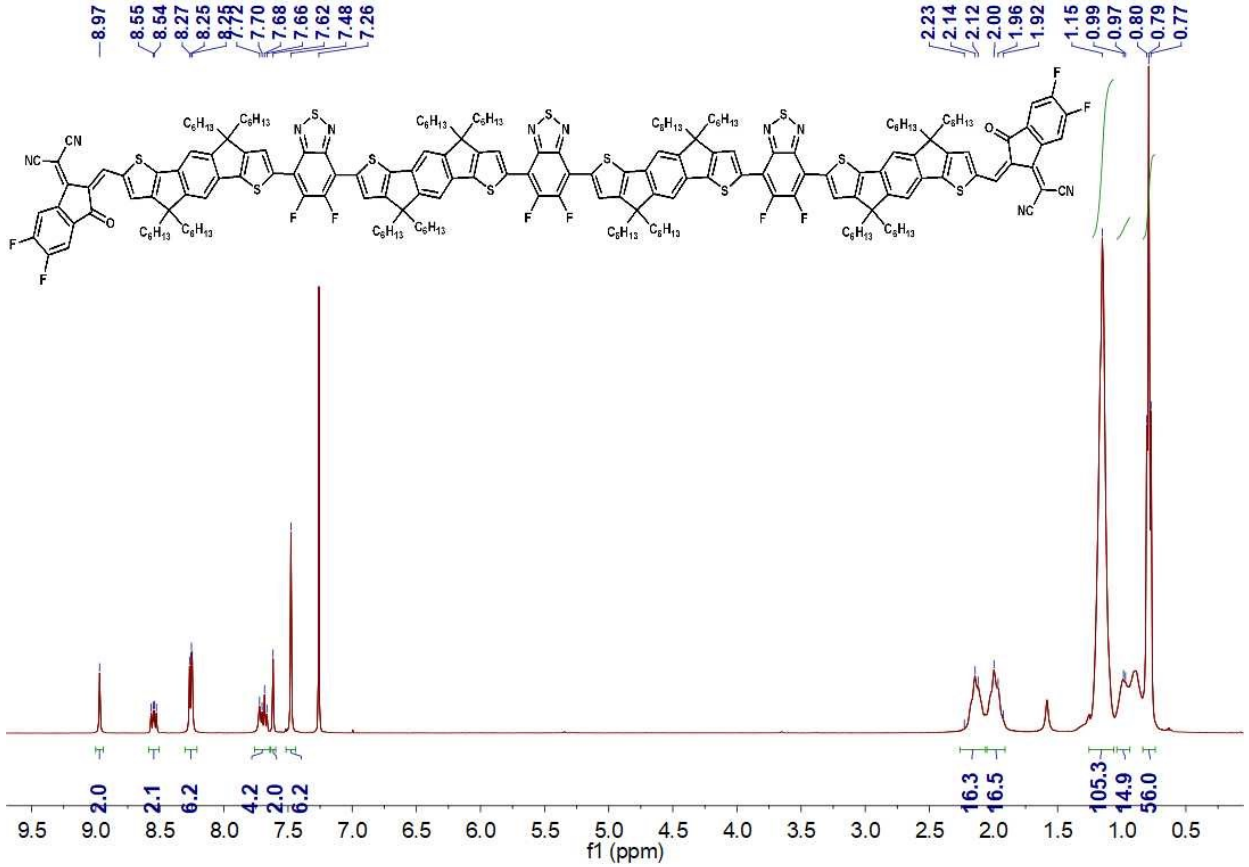

Fig. S31 ^{1}H NMR spectra of IDBF-IC-3 in $CDCl_3$.

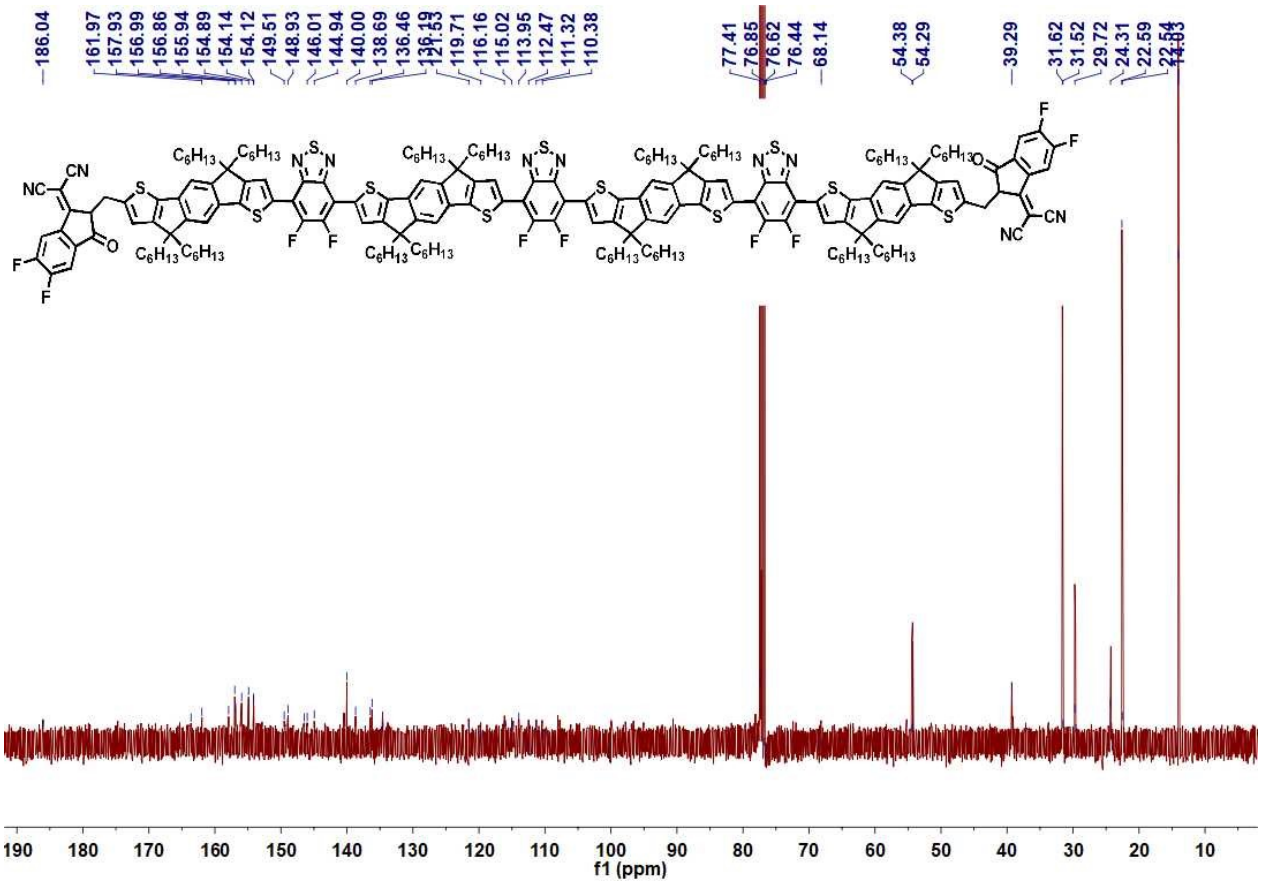

Fig. S32 ^{13}C NMR spectra of IDBF-IC-3 in $CDCl_3$.

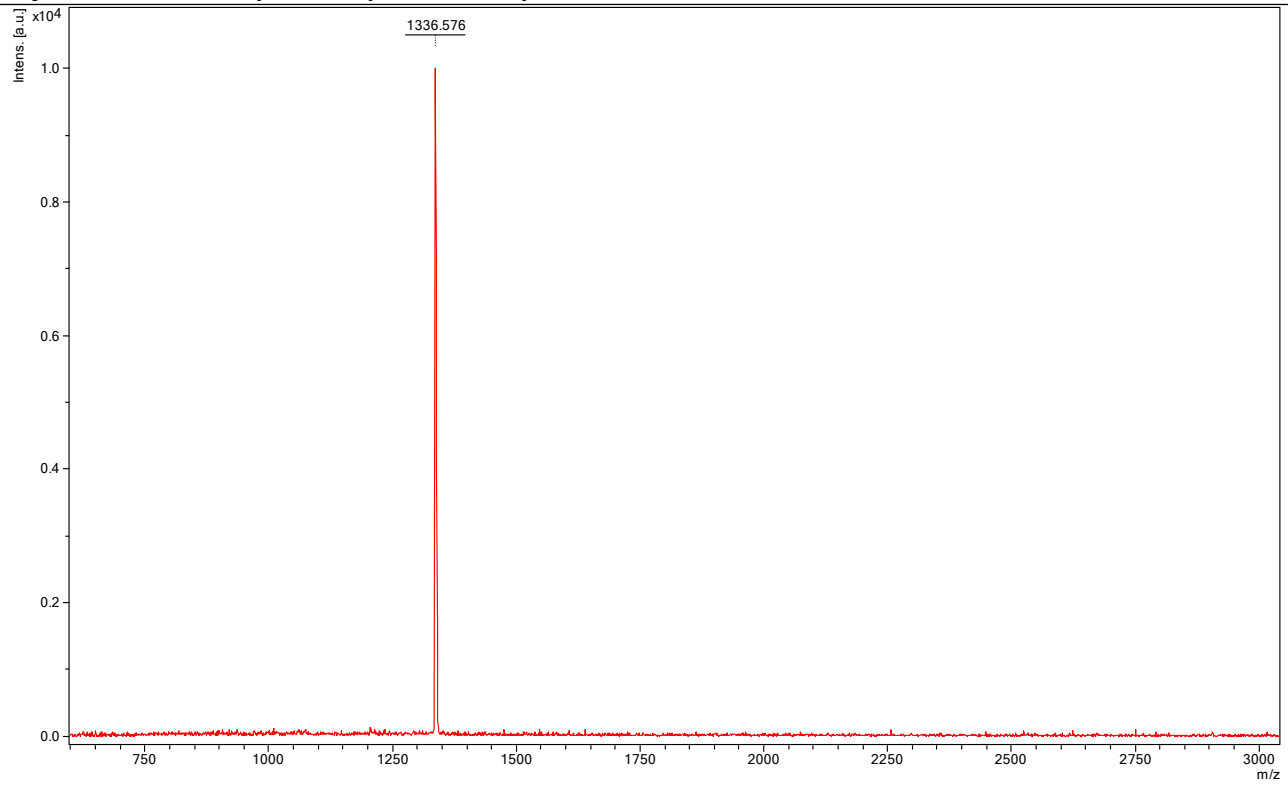

Fig. S33 MALDI-TOF MS spectrum of alt-(IDT-BT)-1**,** calcd. 1336.774, found 1136.576.

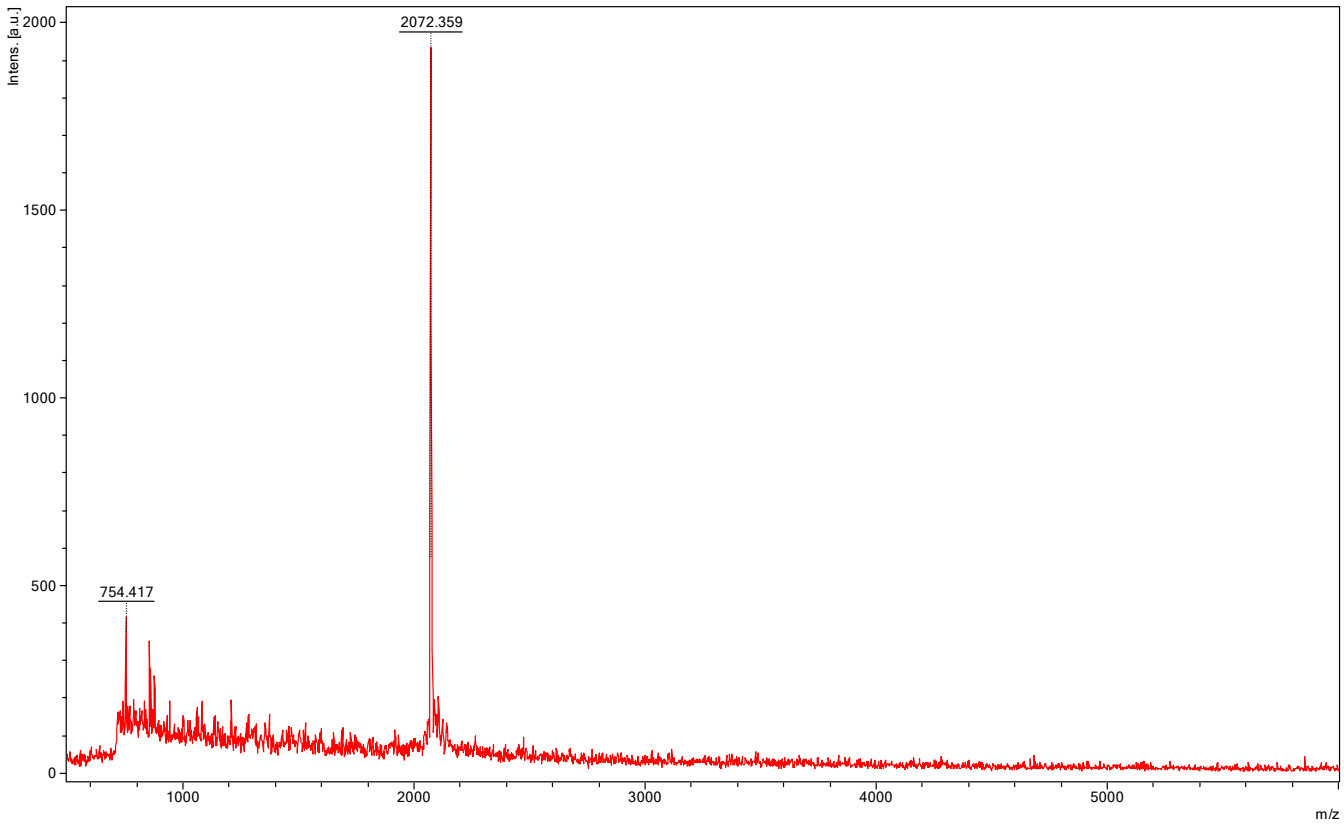

Fig. S34 MALDI-TOF MS spectrum of alt-(IDT-BT)-2**,** calcd. 2072.154, found 2071.359.

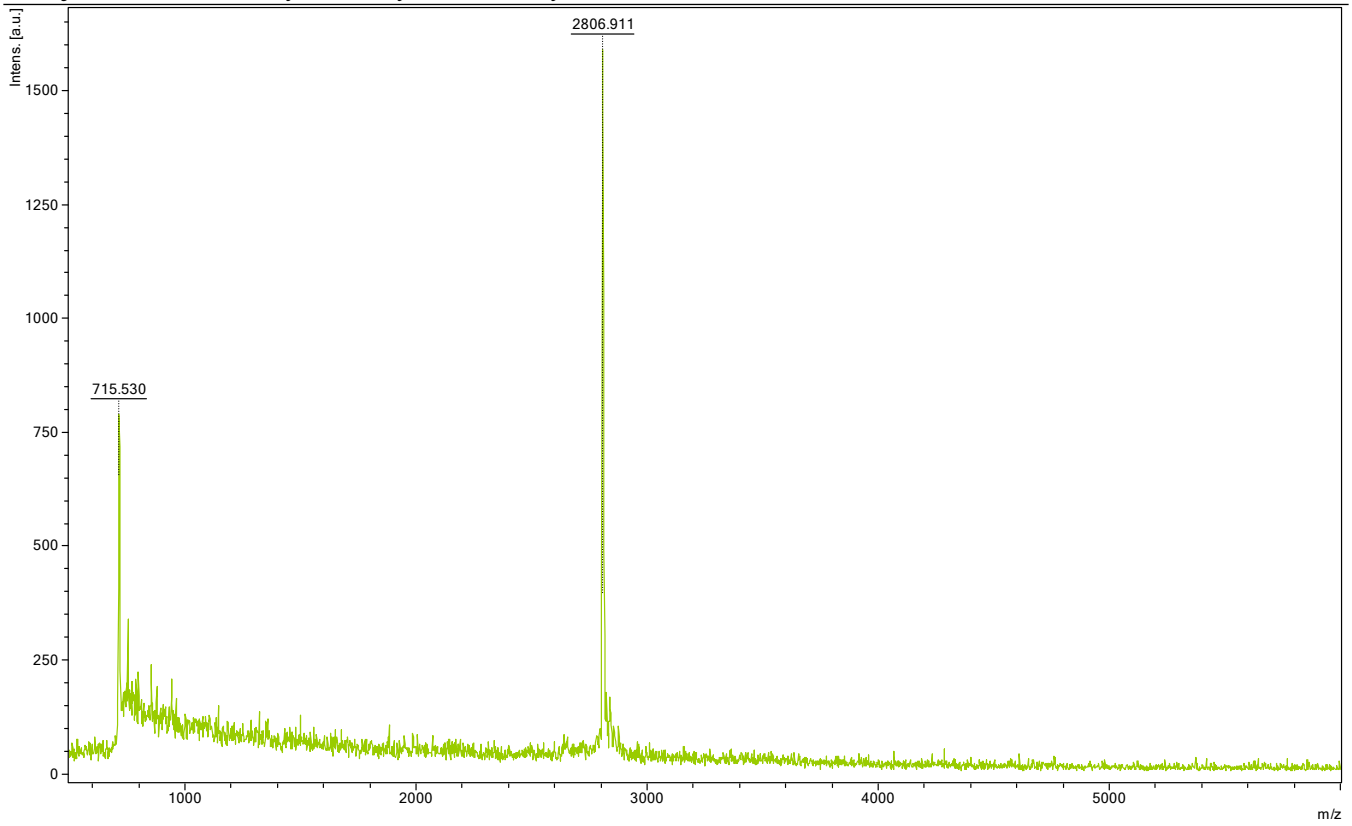

Fig. S35 MALDI-TOF MS spectrum of alt-(IDT-BT)-3**,** calcd. 2806.530, found 2806.911.

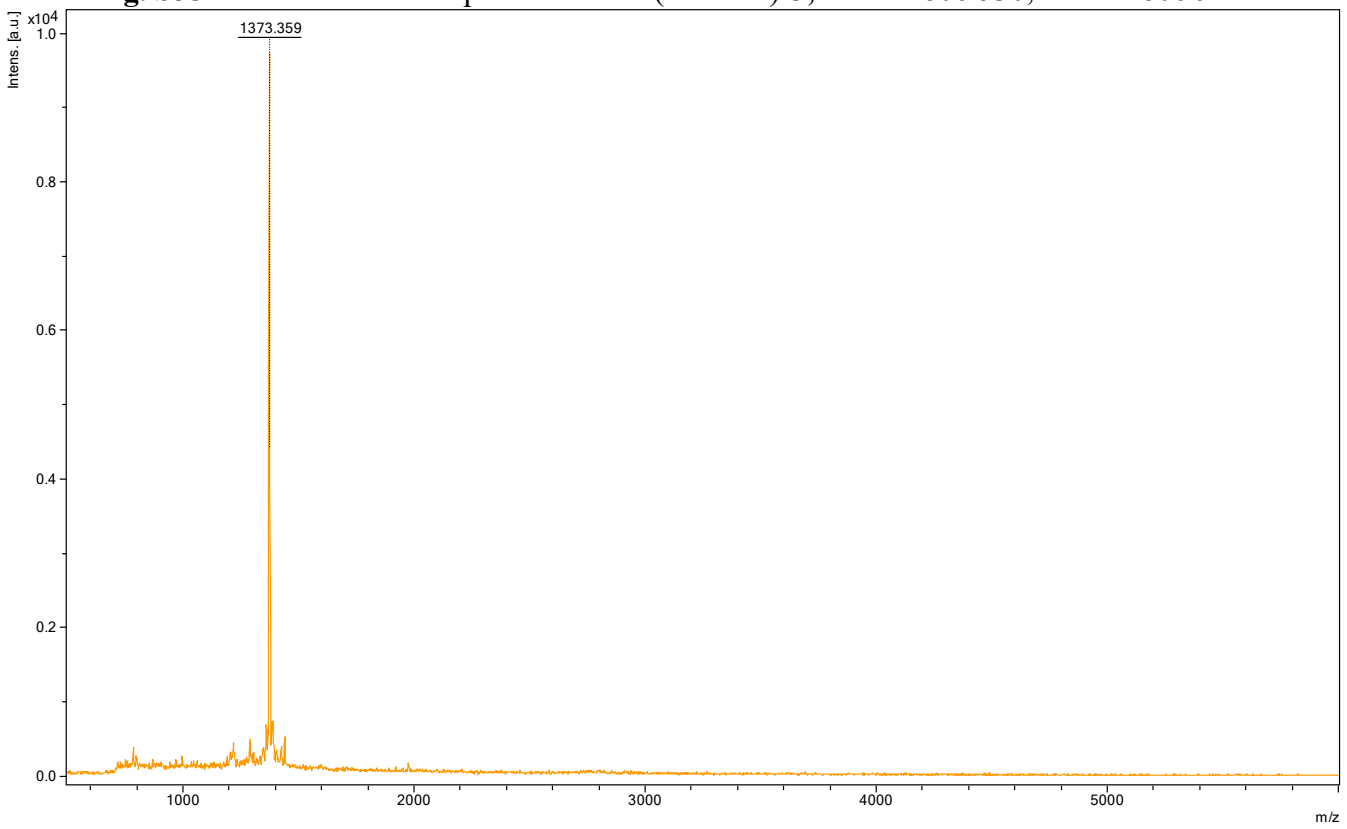

Fig. S36 MALDI-TOF MS spectrum of alt-(IDT-DFBT)-1**,** calcd. 1372.755, found 1373.359.

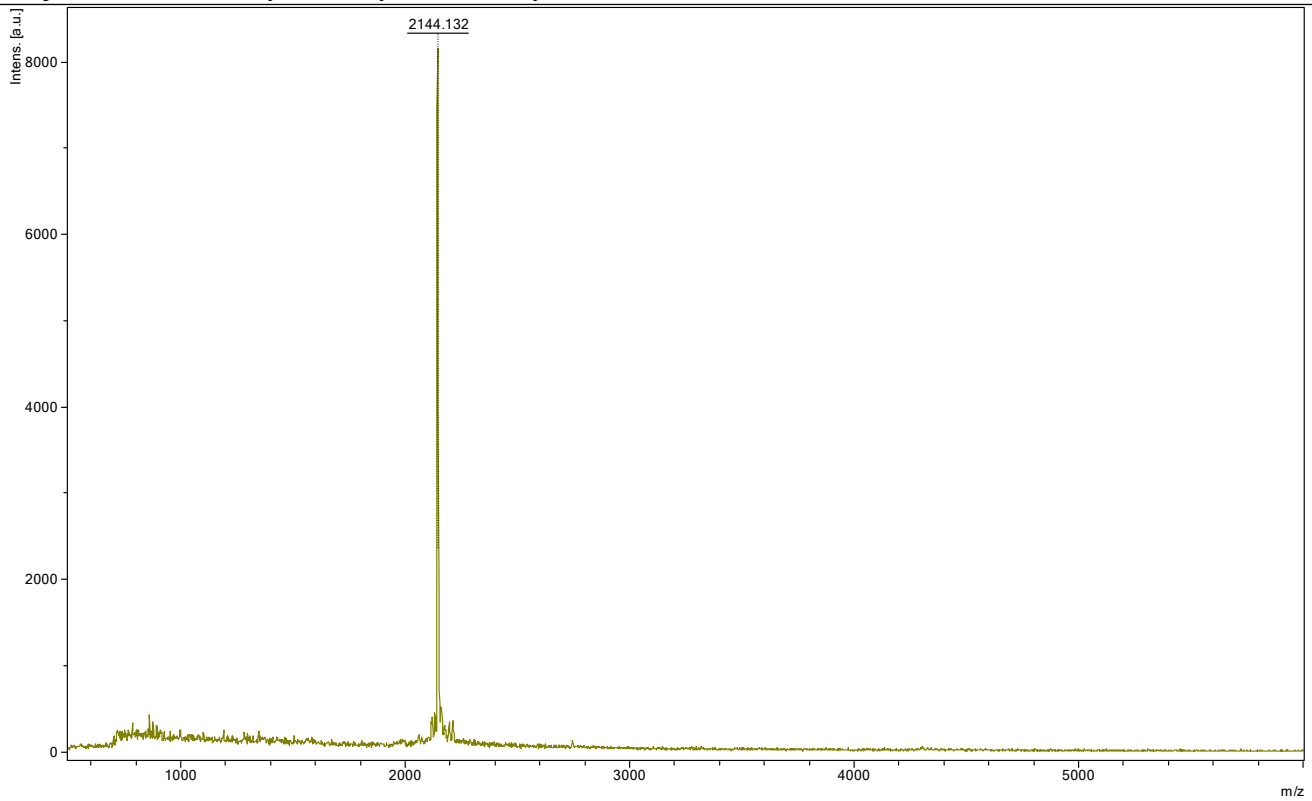

Fig. S37 MALDI-TOF MS spectrum of alt-(IDT-DFBT)-2**,** calcd. 2144.116, found 2144.132.

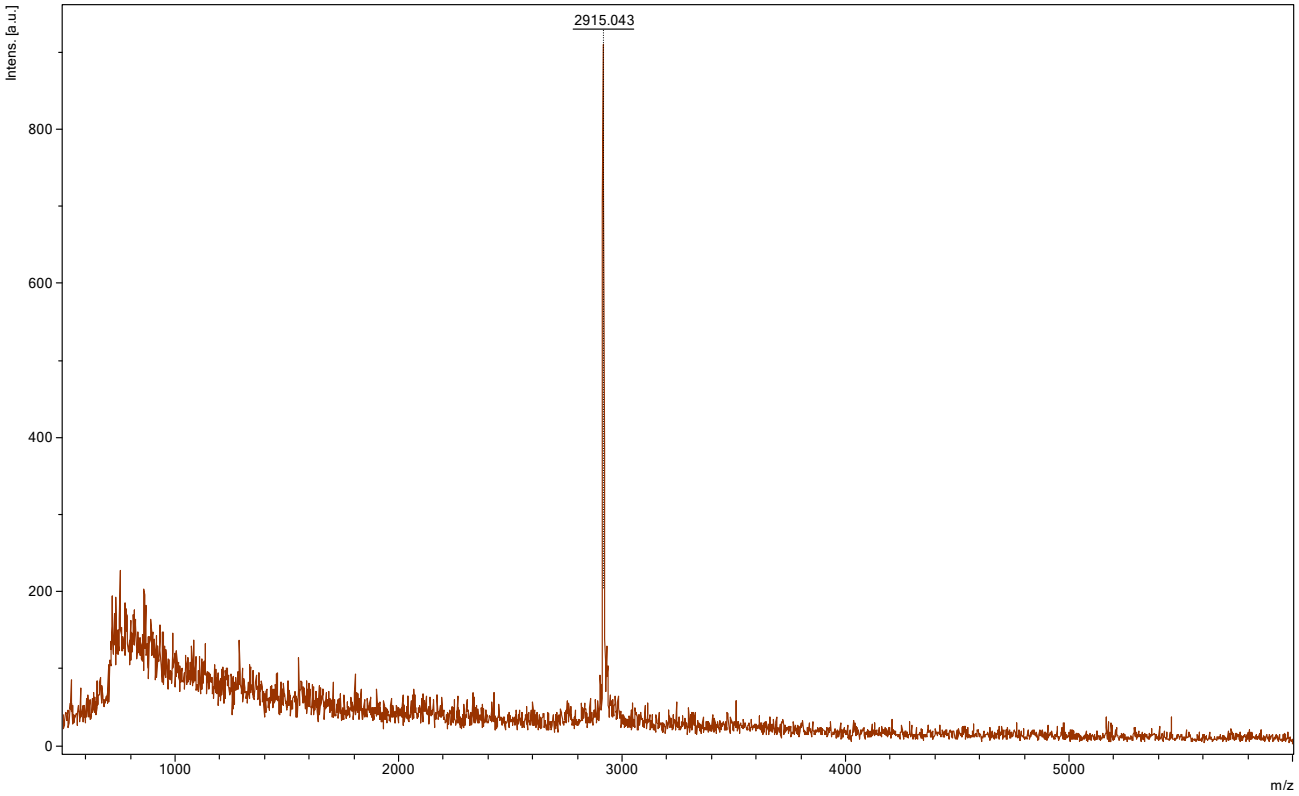

Fig. S38 MALDI-TOF MS spectrum of alt-(IDT-BT)-1**,** calcd. 2914.473, found 2915.043.

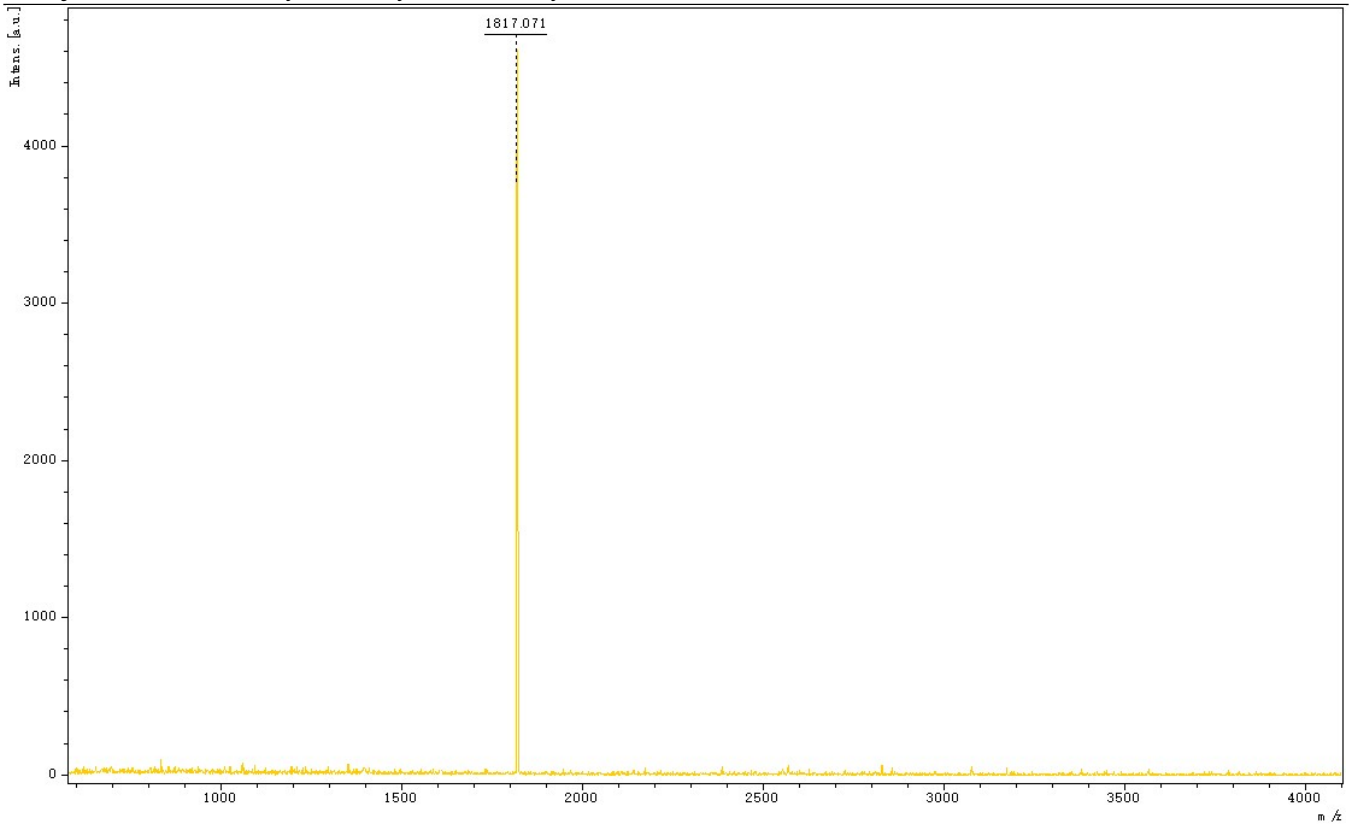

Fig. S39 MALDI-TOF MS spectrum of IDB-IC-1**,** calcd. 1817.804, found 1817.071.

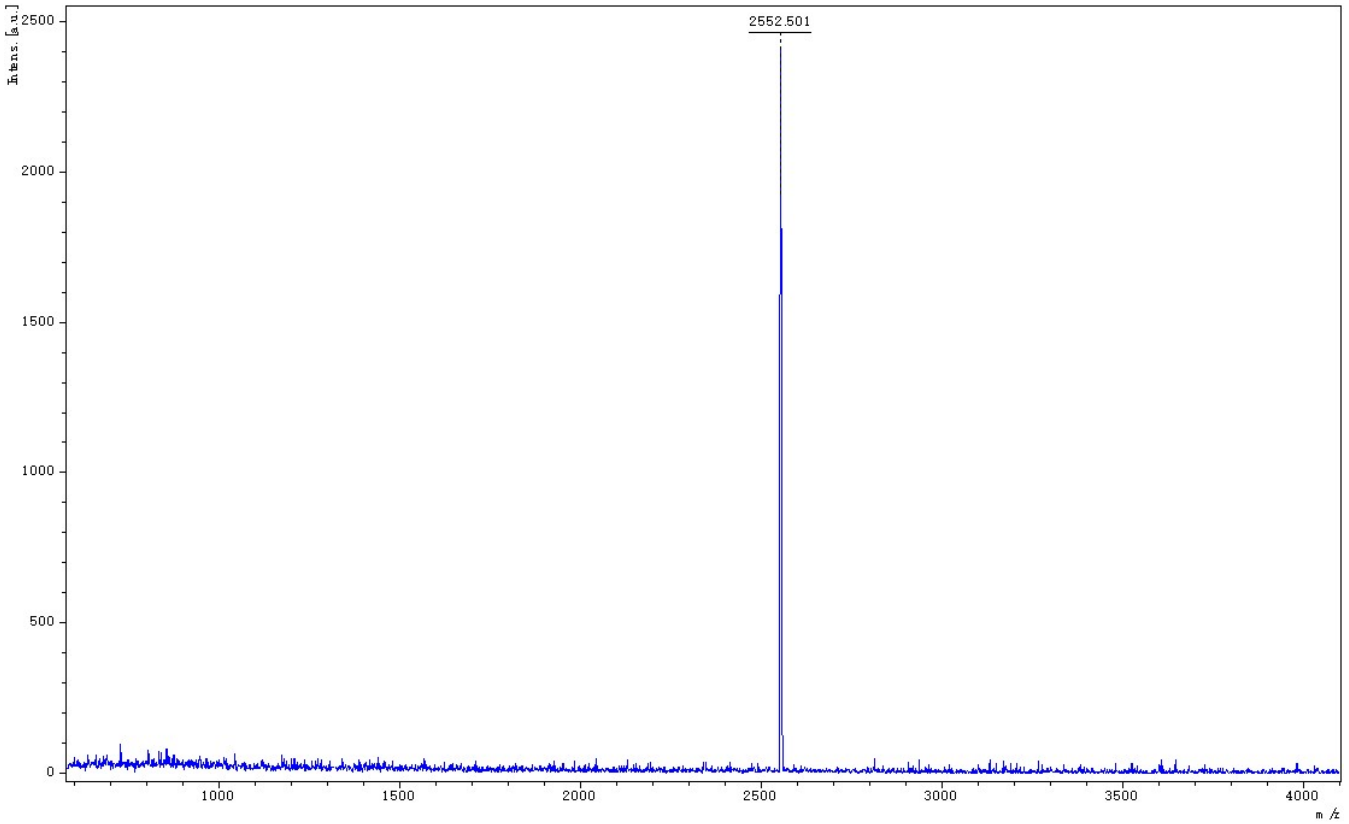

Fig. S40 MALDI-TOF MS spectrum of IDB-IC-2**,** calcd. 2552.181, found 2552.501.

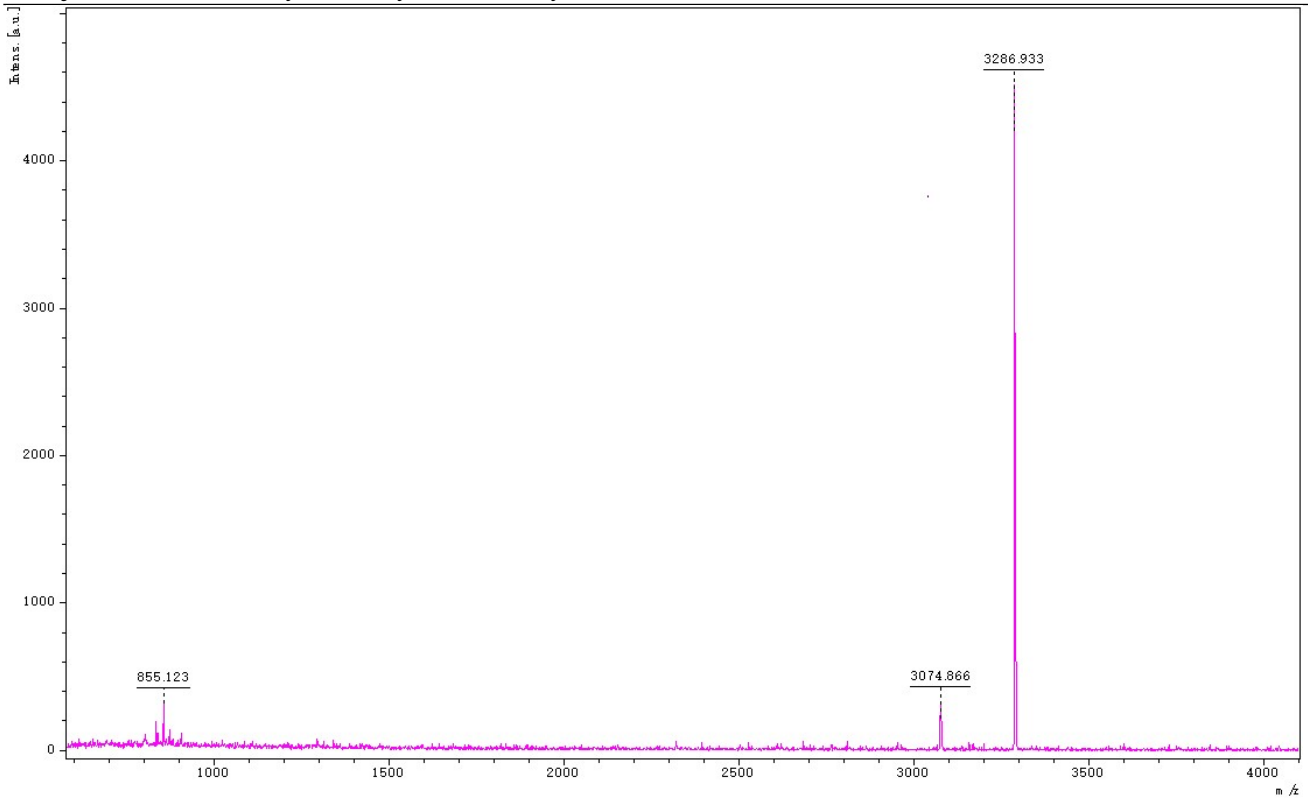

Fig. S41 MALDI-TOF MS spectrum of IDB-IC-3**,** calcd. 3287.56,0 found 3286.933.

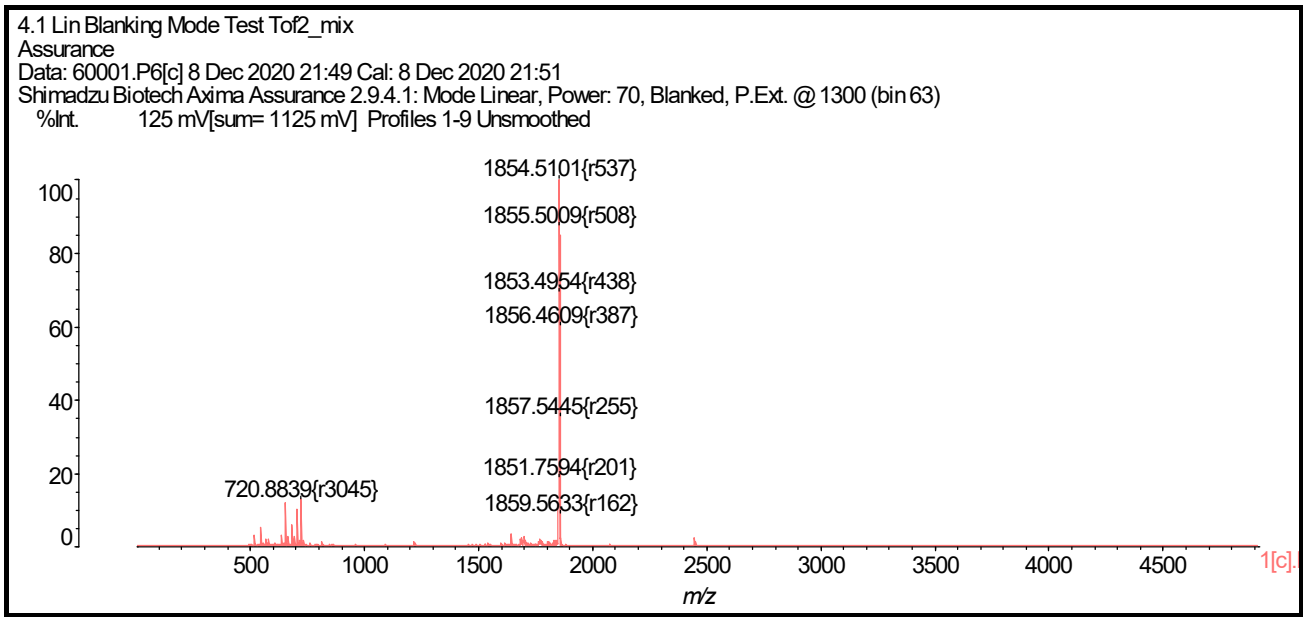

Fig. S42 MALDI-TOF MS spectrum of IDBF-IC-1**,** calcd. 1854.5064, found 1854.5101.

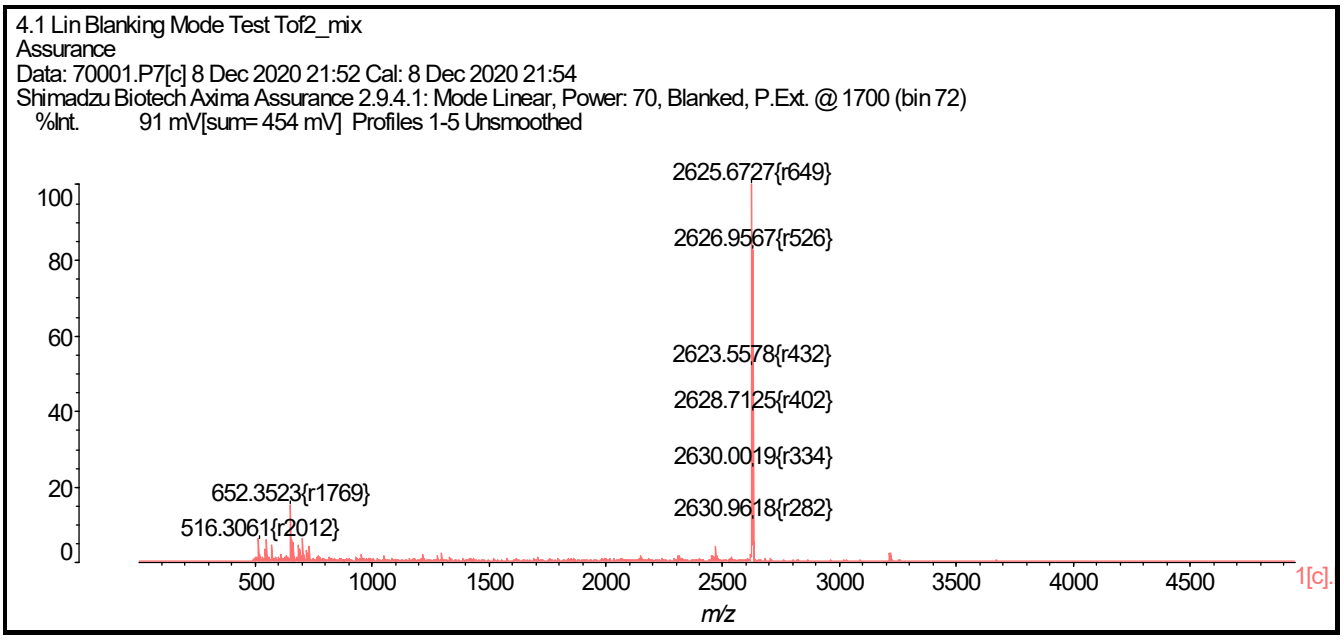

Fig. S43 MALDI-TOF MS spectrum of IDBF-IC-2**,** calcd. 2625.6512, found 2625.6727.

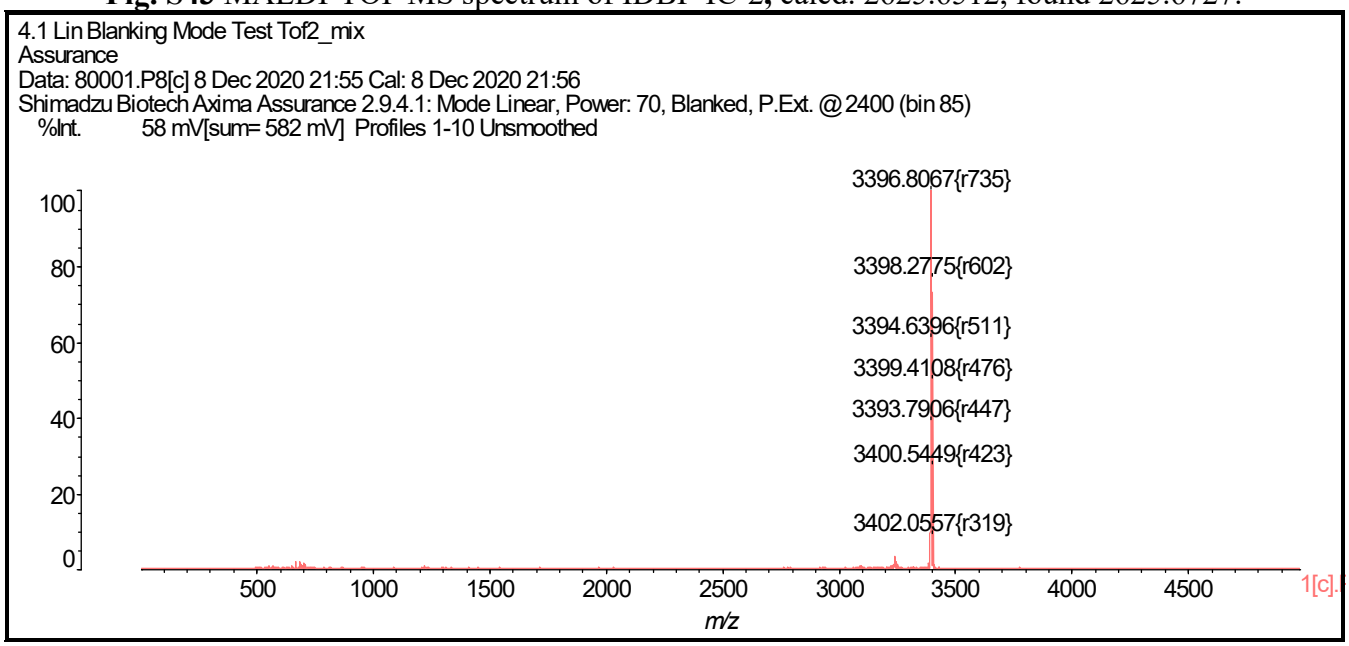

Fig. S44 MALDI-TOF MS spectrum of IDBF-IC-3**,** calcd. 3396.7960, found 3396.8067.